Supplementary information

Material and Methods

Reagents

CAL101 (Idelalisib), AS252424, PI-103 and Leniolisib, were purchased from Selleckem and resuspended in DMSO (Sigma). PLGF (#100-06) and BDNF (#450-02) were purchased from Peprotech. Cytosporone B (#C2997) was purchased by Sigma and resuspended in DMSO. PIK3Cδ (#34050), AURKA (#14475), AKT total (#4691), AKT-Ser473 (#4060) and AKT-Thr308 (#13038), total PDPK1(#3062), Integrin β1 (#9699), S100A4 (#13018) PDGFRβ (#28E1), Caveolin1 (#3267), antibodies were purchased from Cell Signaling; NR4A1 (#STJ94578), mTOR total (#STJ113771) and mTOR-Ser2448 (# STJ27512) and PDPK1-Ser241 (# STJ29323) were purchased from St Johns Laboratory. FAP (#ab54651), α-SMA #ab5694 (α-smooth muscle actin) were purchased from Abcam. PIK3Cδ overexpressing plasmid (pCMV6- PIK3Cδ-AC-GFP) and the empty vector (pCMV6-AC-GFP) were purchased from Origene. All other reagents were purchase from Thermofisher Scientific.

Cell lines and primary samples

MDA-MB-231 were purchased by ATCC, maintained in DMEM low glucose supplemented with 10% FBS and 10 u/ml Penicillin/Streptomycin, incubated at 37 °C with 5% CO_2. BT-549 were purchased by ATCC, maintained in RPMI 1640 supplemented with 10% FBS and 10 u/ml Penicillin/Streptomycin, incubated at 37 °C with 5% CO_2. HMF (Human adult Mammary Fibroblast) were purchased from ZenBio, maintained in E-MEM supplemented with 10% FBS and 10 u/ml Penicillin/Streptomycin and 30 ng/ml of EGF, incubated at 37 °C with 5% CO_2. MRC5 were purchased from ATCC, maintained in E-MEM supplemented with 10% FBS and 10 u/ml Penicillin/Streptomycin and 30 ng/ml of EGF, incubated at 37 °C with 5% CO_2. Matching primary fibroblasts from tumor (< 5cm) or from a distal site (> 5cm) of TNBC patients, were kindly provided by Breast Cancer Now tissue-bank at Bart's Cancer Institute, Queen Mary University, London (patients' information are provided in **Supplementary Table 8**). Primary fibroblasts were grown in DMEM/F12 medium, supplemented with 10µg/ml apo-transferrin, 5µg/ml insulin, 30 ng/ml of EGF, 0.5µg/ml hydrocortisone, 5 µg/ml Amphotericin B, 10% FBS and 10 u/ml Penicillin/Streptomycin.

siRNA transfection

HMF and MRC5 fibroblasts were transfected with a pool of 3 siRNAs targeting each of the 710 human kinases (Silencer Human Kinase siRNA Library, #A30079 Thermofisher). Fibroblasts (1250 cells/well) were seeded in a 96 well plate. 50 nM siRNA/well were used for transfection using 0.8 µl/well of Hi-Perfect (Qiagen) following manufacturer's instructions.

For NR4A1 silencing, the following siRNAs were used: #s144919 and #s41752 (Thermofisher). In addition, non-targeting scrambled control (#AM4611, Thermofisher) was used. Briefly, 400.000 MDA=MB-231 cells were resuspended in 20 µl of complete buffer SE with the addition of 300 nM siRNA. Silencing was then confirmed by real-time qRT-PCR.

For silencing, the following siRNAs were used: PLGF #s10399 and BDNF #s1964 and #s1963 (Thermofisher). In addition, non-targeting scrambled control (#AM4611, Thermofisher) was used. Briefly, 400.000 MRC5 cells were resuspended in 20 µl of complete buffer SE with the addition of 300 nM siRNA, and electroporated using 4D-Nucleofector following manufacturer instruction.

3D co-culture and invasion assay

24 hours after transfection, 2 µl of 0.025% trypsin in 7µl of PBS-EDTA was added to each of the fibroblasts transfected wells. Trypsin action was stopped by adding 30 µl of medium containing 1250 MDA-MB231 cells. Cell suspension was then transferred to an Ultra-low attachment 96 well plate (corning). Plates were centrifuge for 3 minutes at 300xg and incubated at 37 °C for 72 hours. After spheroids formation, 30 µl of Growth factor reduced Matrigel was added to each well, plates were incubated for 2 hours at 37 °C, followed by adding 20% FBS medium to each well to promote invasion. Spheroids pictures were taken after 3 and 6 days using EVOS FL microscope (Thermofisher) and the images were analyzed with ImageJ software. The results were expressed as changes in the overall spheroid surface (Δ=Surface day 6 - Surface day 3).

The Δ-value of each silenced kinase (Δ_K) was compared with the Δ-value of the control (Δ_{CT} of the non-targeting/scrambled siRNA), at different time-points, to obtain a Δ_{Ratio} ($\Delta_{Ratio}=\Delta_{CT}/\Delta_K$). Kinases with a $\Delta_{Ratio} \leq 0.5$ (50% less invasion vs CT) were considered as 'invasion promoting kinases', (as their silencing led to a reduction of invasion), while kinases with a $\Delta_{Ratio} > 2$ (100% more invasion vs CT) were considered as 'invasion inhibiting kinases', (as their silencing led to an increase of invasion). Based on our cut-off values/criteria, we classified kinases with Δ_{Ratio} between 0.5 and 2 as 'uninfluential on the invasiveness of MDA-MB-231 cells. The Δ_{Ratio} values were used to calculate the Z-Scores based on the formula: $z = (x - \mu)/\sigma$ (μ: Δ_{Ratio} mean of 710 kinases; σ: standard deviation (SD); x: Δ_{Ratio} value for each kinase).

Screening validation

MRC5 cells (50.000/well) were seeded in a 24well plate. Using Fugene HD (Promega), cells were transfected with 0.5 µg/well of pLKO.1-puro Vector empty or with plasmids containing the target shRNA sequence for the indicated kinases (Mission Library, Sigma). 48h after transfection, cells were counted for 3D co-culture with MDA-MB-231 and subsequent invasion assays were performed as described above. Part of the transfected cells were used to determine the efficacy of silencing using

Cells To CT kit (Thermofisher), following manufacturer's instruction for Real-time PCR assay (qRT-PCR), using specific primers for each silenced kinase (QuantiTect, #249900, Qiagen).

Lipophilic tracer staining and Real-time 3D invasion assay

SP-DiOC18(3) or Dil Stain (Thermofisher) were added to 10^6 cells in serum-free medium to a final concertation of 5 µM. Cells were then incubated at 37°C for 1h, and centrifuged for 5 minutes at 300xg and washed twice with PBS. Finally, cells were resuspended in fresh complete medium and used for further assays.

Western Blotting

Cells were dissolved in RIPA Buffer (Sigma), as previously described (1). Protein concentration was measured by BCA Protein Assay Reagent Kit (Pierce, Rockford, IL, USA), as described (2). Proteins were fractionated on 10% SDS-PAGE, and transferred by electrophoresis to Nitrocellulose Transfer Membrane (GE). Membranes were incubated with several primary antibodies. Horseradish peroxidase-conjugated antibody anti-mouse IgG and anti-rabbit IgG (Dako) were used to detect immunoreactive bands and binding was revealed using enhanced chemiluminescence (Pierce). The blots were then stripped and used for further blotting with anti-GAPDH antibody (Thermofisher #AM4300). Unless otherwise specified, displayed western blots are representative images of at least 2 independent experiments.

Where indicated densitometric analysis of detected bands were performed by measuring the peak height of the bands using ImageJ and normalized using loading control.

2D Invasion Assay

Reduced growth factors Matrigel (BD Biosciences) was polymerized in 8 µm pore cell inserts (Sarstedt) prior to the addition of cells. MDA-MD-231 or BT549 ($5x10^4$) cells were seeded into the insert containing Matrigel in serum free media. Fibroblast, pre-treated with CAL101 or DMSO for 24h were used as an attractant in the bottom chamber, and cells were allowed to migrate for additional 24 h, the inserts were then removed and migrated cells were fixed with PFA 4% and then stained with crystal violet and counted providing a quantitative value for migrated cells across the membrane.

Real-time invasion assay

MDA-MB-231 and BT-549 TNBC cell lines were seeded in cell inserts with 0.4 µm pores, to be co-cultured with fibroblasts pre-treated with 10 µM CAL-101 or vehicle only. 24h after co-culture, TNBCs were collected and counted and used for real-time invasion assay. Cell invasion was monitored in real time using the xCELLigence RTCA technology as previously described (3). CIM-16-well plates, provided with interdigitated gold microelectrodes on bottom side of a filter membrane

interposed between a lower and an upper compartment, were used. The lower chamber was filled with 10 % serum- medium, cells (2×10^4 cells/well) were seeded on filters in serum-free medium. Microelectrodes detect impedance changes which are proportional to the number of invading cells and are expressed as cell index. Invasion was monitored in real-time for at least 30h. Each experiment was performed at least twice in quadruplicate.

Conditioned medium preparation

HMF and MRC5 were seeded in 10 cm plates and treated with either vehicle or with 10 μM CAL-101 or transfected to silence or overexpress PIK3Cδ, in serum free for 24h in order to obtain the conditioned medium (CM). Medium collected was centrifuged for 30' at 1800 x g at 4°C and then passed through a 0.22μm filter, aliquoted and store at -80°C for further assays.

PIK3Cδ overexpression and silencing

MRC5 cells were transfected with pCMV-PIK3Cδ-AC-GFP (Origene) or empty vector using 4-D electroporator (LONZA), following manufacturer instruction. Briefly, 400.000 cells were resuspended in 20 μl of complete buffer SE (Lonza), and 0.4 μg of plasmid DNA were added prior electroporation, cells were then seeded in warm complete medium. Similarly, for PIK3Cδ siRNAs (s10531, s224263, s10530 Thermofisher) or scramble control (AM4611, Thermofisher), 400.000 MRC5 were resuspended in 20 μl of complete buffer SE with the addition on 300 nM siRNA. For short hairpin RNA (shRNA) silencing, pLKO.1-puro Vector empty or containing the target shRNA sequence for PIKCδ (Mission Library, Sigma) were transfected using 4-D electroporator (LONZA), following manufacturer instruction. Briefly, 400.000 cells were resuspended in 20 μl of complete buffer SE (Lonza), and 0.4 μg of plasmid DNA were added prior electroporation, cells were then seeded in warm complete medium. Overexpression and silencing were then confirmed by real-time qRT-PCR.

RNA extraction and Real-time qRT-PCR

Total RNA was extracted from the cell lines using PureLink RNA Mini Kit following the manufacturer's instructions (Invitrogen). All RNA samples were subjected to DNase I treatment. The RNA samples were subjected to RT using SuperScript IV VILO following the manufacturer's instructions (Invitrogen). Real-time quantitative RT-PCR (qRT-PCR) was performed to assess the expression of human PIK3CD (Hs00192399_m1) using the TaqMan gene expression assay (Applied Biosystems) while GAPDH was used as reference (Hs99999905_m1). For RNAseq validation, Real-time PCR assay (qRT-PCR), was performed using specific primers for each silenced kinase (**Supplementary Table 4**). The samples were run in triplicate on an Applied Biosystems STEPONE thermal cycler and analyzed with the SDS 1.9 Software (Applied Biosystems), by applying the

method described by Pfaffl and previously applied (4, 5).

Cell viability

Cell viability assay was performed as previously described (2) (6). Briefly, cells were seeded in 5.000 for well in a 96 well plate and treated with the indicated compound and time points and cell viability was evaluated by Cell Titer-Glo 2.0 (Promega) according to manufacturer instruction. 6 replicates in 3 independent experiments were analyzed and results were expressed as percentage mean ± SEM vs vehicle treated cells.

Statistical analysis for cell based assay

Statistical analysis was performed using GraphPad Prism software. Specific statistical tests are described in figure legends, two-tails t-test was applied where indicated. Unless otherwise specified, all the graphs displayed represent a distribution of all recorded measures in the different experiments normalized for the control(s).

Secretome analysis

Supernatants of CAL-101 and Vehicle (DMSO)-treated fibroblasts were collected after 24 h incubation in serum free MEM. Supernatants were dialyzed and after quantification, secreted proteins were biotin-labelled and hybridized onto human L1000 glass slide arrays (RayBiotech; https://www.raybiotech.com/human-l-1000-array-glass-slide-2). Detected fluorescence signals were then normalized to positive controls.

RNA Extraction, Library Construction and RNA-Sequencing

Cell pellets were obtained from MDA-MB-231 co-cultured in 6-well cell inserts with MRC5 treated with CAL-101 10 µM or vehicle only. All conditions were analyzed using 2 biological replicates. RNA was extracted as described before (6). The RNA samples were then quantified using a Qubit 2.0 (Life Technologies, CA, USA) fluorimeter from Invitrogen with a high sense RNA kit. The quality of RNA was assessed and confirmed using the RNA Pico 6000 kit. The high-quality RNA were then used for library preparation using the RNA hyper prep kit with riboerase from the KAPA Biosystems (Cat. No. KK8560) according to the manufacturer's recommendation and were fragmented at 85˚C for 4.5 minutes. The libraries were amplified using 8 cycles of PCR and were ligated with the NEXTflex-96 DNA barcodes (Bio Scientific). The library was quantified using the Qubit DNA high sense kit, and its quality was confirmed using Bioanalyzer (DNA high sense kit). Libraries were then pooled and diluted to a final concentration of 2nM. Pooled and diluted library were denatured along with 1% PhiX spike in as per recommendation from Illumina. Library was loaded onto the NextSeq 550 v2 mid-output 150 cycle kit.

Raw data processing, alignment analysis, and identification of differentially expressed genes

We first obtained the high-quality clean reads by trimming the adapter sequences and removing reads that contained poly-N or were of low-quality from the raw data using the fastX tool kit (v 0.0.14) (http://hannonlab.cshl.edu/fastx_toolkit/license.html). The quality of reads were then confirmed using the fastqc tool kit (v 0.11.5) (http://www.bioinformatics.babraham.ac.uk/projects/fastqc/). The downstream analyzes were conducted using this high-quality clean read. Briefly, the high-quality reads were mapped to the ENSEMBL built GRCH37 using the STAR aligner (v2.5.3a) (7) with the ENCODE options as described in the STAR manual. We then estimated the read counts for each gene using the summarize Overlaps function provided with the R package DESeq2 (8). Consequently, we performed differentially expressed genes (DEGs) using DESeq2 non-interaction model and the Benjamini-Hochberg corrected *P* value ($P_{adj} \leq 0.05$) and Log2 fold change $\geq |0.5|$ were used as the threshold to screen significance of DEGs. The pathway analyzes for the secretome data and the RNAseq data combined were performed using the Ingenuity Pathway (https://www.qiagenbio-informatics.com/products/ingenuity-pathway-analysis).

Sequencing data availability

RNA-seq data have been submitted to the NCBI Bioproject Database (submission ID SUB7028041, BioProject ID PRJNA608606)

Functional annotation of secreted proteins

Analyzes to identify canonical pathways effected by CAL-101 treatment of the HMF and MRC5 cells was conducted by using secreted proteins differentially expressed in comparison to CAL-101 treatment and the Ingenuity Pathway Analysis tool (https://www.qiagenbio-informatics.com/products/ingenuity-pathway-analysis).

Xenograft mouse model

Animals were obtained from Charles Rivers (Italy). All mice were kept in the animal facilities of BSRC "Alexander Fleming" under specific pathogen-free conditions. The experiment was performed with mice aged 8 weeks. All procedures were approved by the Prefecture of Attica (license #3554/2018) in accordance to national legislation and the European Union Directive 63/2010. The study consisted of 4 experimental groups each containing 10 female NOD SCID mice after randomization. On day 0, $1x10^6$ MDA-MB-231-Luc cells or $1x10^6$ MDA-MB-231-Luc with $1.5x10^6$ MRC5 cells, respectively, in 200μl Matrigel:PBS 1:1 were injected in the mammary fat pad of 20 animals per condition. Primary tumor sizes were measured twice weekly (Monday and Friday) by calipering. Tumor volumes were measured every 3 or 4 days using a calliper and calculated using the

formula: W2xL/2 (L= length and W= the perpendicular width of the tumor. On day 7, after mean tumor volumes had reached approx. 100-200 mm^3, animals were randomized into 4 groups per condition, each containing 8 animals. On the same day, treatment with 2 mg/kg CAL-101 orally was initiated for Groups 2 (MDA-MB-231+CAL-101) and 4 (MDA-MB-231+MRC5 +CAL-101), whereas animals of Groups 1 (MDA-MB-231) and 3 (MDA-MB-231+MRC5) were kept untreated (vehicle; 30% PEG 400 +0.5% Tween 80). Animals of Groups 2 and 4 were treated for 10days. Mice were sacrificed on day 28. Primary tumor tissues of all animals were photographed and collected and wet weights and volumes determined accordingly. Fifteen minutes prior to bioluminescent imaging, all mice were intraperitoneally injected (150 mg/kg) with a 30 mg/ml solution of D-luciferin (Vivo Glo Luciferin, P1043, Promega) in PBS. Quantitative imaging of bioluminescence was performed, using the In-Vivo Xtreme Imaging System (Bruker).

Histology and immunohistochemistry of xenograft tissues

At the end of the study, one half of every tumor was fixed in formalin 10% (pH = 6.9–7.1) O/N at 4°C before processing for paraffin embedding and the other half was embedded in Optimun Cutting Temperature compound (VWR chemicals). At least 2 serial sections of 5 μm were stained with: hematoxylin and eosin (H&E) for general histology. For Ki67 staining, paraffin embedded tissues sections were deparaffinized, hydrated, and treated with boiling Citrate buffer pH 6.0 under microwaves for 20 min. Sections were blocked in 2% BSA. Primary monoclonal antibody Ki67 (SP6, Thermofisher) and HRP-conjugated secondary antibodies (Southern Biotech) were incubated in diluent for 1–24 h. Visualization was performed with DAB (Vector) and counterstained with hematoxylin; Photomicrographs were acquired using a Nikon ECLIPSE E200 microscope equipped with a Nikon Digital Sight DS-5M digital camera.

For immunofluorescent staining, 4μm frozen sections were fixed in 4% paraformaldehyde or cold acetone for 10 minutes, permeabilized with 0.2% Triton X-100 for 30 min and blocked with 5% BSA for 1 hour. Primary antibodies (anti-fibroblasts clone TE-7, Millipore and phospho AKT/4060 Cell Signaling) were diluted in 3%BSA and incubated overnight at 4°C. Then, samples were washed with PBS-0.05% Tween-20 and incubated with fluorescent-conjugated secondary antibody (Alexa 488-conjugated mouse and rabbit antibody; Invitrogen) for 1hour. All samples were counterstained with DAPI. Photomicrographs were acquired using Leica Fluorescent Microscope (Leica DM 2000).

MMTV-PyMT transgenic mouse model

Four-week-old MMTV-PyMT transgenic mice under pathogen-free conditions were administered with either 10 mg/kg body weight of the selective PIK3Cδ inhibitor CAL-101 (#S2226, Selleckchem) or the control vehicle by daily oral gavage for 6 weeks. At the age of 10 weeks, mice (n=4 / group)

were harvested and the mammary tumors, lungs and livers were fixed in 4% paraformaldehyde and embedded in paraffin.

TCGA BC dataset deconvolution pipeline

We estimated the specific expression of different PIK3C isoforms in fibroblasts in different BC subtypes (including ERα+, HER2+ and TNBC) RNA-seq samples from TCGA (https://portal.gdc.cancer.gov/projects/TCGA-BRCA) by applying a recently developed deconvolution algorithm CDSeq (https://github.com/kkang7/CDSeq) to the bulk RNA-seq samples of 1051 BC patients. First, we downloaded the RNA-seq HTSeq read count data for those samples from the TCGA data portal (https://portal.gdc.cancer.gov); we performed no additional normalization. Next, we extracted the read counts value for 45 known breast-cancer-associated fibroblast (CAF) marker genes (compiled from Le Bleu et. al. (9)) and 547 immune marker genes for various immune subtypes based on a reference profile developed by CIBERSORT (10) (**Supplementary Table 13**). Next, we used CDSeq to estimate the proportions of CAFs in each of the 1051 samples and the corresponding cell-type-specific gene expression profiles (GEPs). We set the number of cell types to 20 (which should be large enough to detect the major cell types in the data). CDSeq identified four CAFs in which the CAF marker genes had 1.5-fold or higher expression compared to expression of immune marker genes. Then, for each BC sample, we estimated CAF-expressed PIK3C-isoforms' expression levels by multiplying the PIK3C-isoform expression level in four CDSeq-estimated CAFs expressions with their estimated proportions. Finally, we analyzed the association between the different BC subtype patients' survival time and their estimated CAFs-expressed PIK3C-isoforms'levels. Samples were grouped into "High CAF-PIK3C isoform' if their CAFs-expressed PIK3C isoform levels were above the 60th percentile of CAFs-expressed PIK3C isoform levels of all samples, and into "Low CAF-PIK3C isoform" if their CAFs-expressed PIK3C isoform levels were below the 40th percentile. For the survival analysis, we employed a MATLAB function MatSurv (https://github.com/aebergl/MatSurv) which generates a Kaplan-Meier plot and calculates the estimated Hazard Ratio (HR) and associated p-value (log-rank test).

Immunohistochemistry and immunofluorescence staining of transgenic tissues

Paraffin-embedded samples were sectioned at 4 μm thickness. Antigen retrieval was performed by incubation of the slides in a pressure cooker for 5 min in 0.01 M citrate buffer, pH 6.0, and subsequent treatment with 3% hydrogen peroxide for 5 min. Slides were incubated overnight at 4 °C with antibodies to the following: α-SMA (Abcam, ab21027, 1:00), F4/80 (Biolegend, 123101, 1:20), PIK3Cδ (Santa Cruz, sc-55589, 1:30), pAkt-S473 (Cell Signaling Technology, CST, 4060, 1:100), pAkt-Thr308 (Millipore, 07-1398, 1:100), E-cadherin (CST, 14472S, 1:100), Vimentin (CST, 5741S,

1:100), CD31 (Abcam, ab9498, 1:100), Ki67 (Abcam, ab15580, 1:50). Immunohistochemical staining was performed according to the manufacturer's instructions. For immunofluorescence, specimens were incubated with Alexa Fluor secondary antibodies (Thermo Fisher Scientific, A-31571, A-31570, A-31572, and A-31573) for 1 hr at room temperature. DAPI was then used for counterstaining the nuclei and images were obtained by laser scanning confocal microscopy (LSM780, Zeiss).

Clinical specimens

This study was conducted on n=179 TNBC cases with (n=86) or without (n=93) Lymphovascular Invasion (LVI) from patients presenting at Nottingham City Hospital (11, 12). Treatment and outcome data, including BC-overall survival (OS) and Disease-Free survival (DFS) was maintained on a prospective basis. OS was defined as the duration (in months) from the date of primary surgery to the patients' survival at the end of follow up time. DFS was defined as the duration, in months, from primary surgical treatment to the occurrence of first local, regional, or distant metastasis.

The sample set of the ERα^{+} cohort (n=73) were newly diagnosed BC patients presenting at the National University Cancer Institute, Singapore who were treated with primary or neoadjuvant chemotherapy or endocrine therapy before surgery. Baseline tumor biopsies were taken before anti-cancer therapy and analyzed. All patients in this study provided written informed consent to be enrolled; the studies were approved by the local ethics review committee.

Immunohistochemistry of clinical samples

PIK3Cδ protein expression was evaluated by immunohistochemistry (IHC) using the rabbit PIK3Cδ antibody (PA5-15250; ThermoFisher Scientific) in full-face FFPE breast cancer tissue sections using either the Novolink Max Polymer Detection system (Leica, Newcastle, UK) for the Nottingham TNBC cohort, or the Leica Bond Max automated system (Leica Biosystems, Nussloch GmbH) using the bond polymer refine detection kit (DS9800, Leica Biosystems). The antibody was incubated for 1 hour at a concentration of 1:100. PIK3Cδ cytoplasmic immunoreactivity in the invasive tumors cells was assessed using the modified Histo-score (H score) method (13). Surrounding fibroblasts were identified by IHC expression of α-SMA (Abcam, ab5694) in serial FFPE sections. The antibody was incubated for 1 hour incubated using a 1:500 concentration. As the intensity of PIK3Cδ was not variable in inter-tumoral fibroblasts, it was assessed as a percentage of positively-stained cells.

Statistical analysis of clinical samples

IBM SPSS 22.0 (Chicago, IL, USA) software was used for statistical analysis. The H-scores of tumoral PIK3Cδ expression did not follow a normal distribution and expression of PIK3Cδ protein was dichotomized using the median and the cut point derived from prediction of patient survival using

X-tile (http://tissuearray.org; Yale University), with OS as the endpoint. Both gave a similar result with the strongest significance with outcome seen with the X-tile cut point.

Analysis	X-tile P value	Median P value
TNBC Fibroblast-PIK3Cδ (Overall Survival)	0.000285	0.007
TNBC Fibroblast-PIK3Cδ (Disease Free Survival)	0.048	0.021
TNBC Tumoral-PIK3Cδ (Overall Survival)	0.0004	0.020
TNBC Tumoral -PIK3Cδ (Disease Free Survival)	0.009	0.054

Kaplan–Meier and log-rank analysis were used to assess OS and DMFS. Multivariate Cox Regression analysis with adjustment of covariates was fitted to test independence from standard prognostic factors in breast cancer (tumor grade, tumor size, lymph nodal stage, age, and LVI status) was used to identify independent prognostic value. Spearman's correlation coefficient was carried out to examine the association between PIK3Cδ in the tumor and surrounding fibroblasts. P value ≤ 0.05 was considered significant.

Supplementary Figure legends

Supplementary Figure 1: **CAF markers in primary and immortalized fibroblast cell lines and expression of PIK3Cδ in fibroblasts and breast cancer cell lines.**

(A) Western blotting of CAF markers in HMF, MRC5 and in matching fibroblasts obtained from four TNBC patients (CAFs<5cm; NFs >5cm distance from the tumor site). GADPH was used as loading control. **(B)** PIK3Cδ expression in fibroblasts (primary and immortalized cell lines). GAPDH was used as loading control. (**C**). Comparison of PIK3Cδ expression in breast cancer cells and primary fibroblasts. α-Tubulin was used as loading control.

Supplementary Figure 2: 3D spheroid formation and invasion of fluorescently labelled cells.

Representative image showing the distribution of fluorescently labelled fibroblast and TNBC cells. During spheroids formation, fibroblast (green; SP-DiOC18) and TNBC cells (red; Dil Stain) form a compact agglomerate, making it difficult to distinguish between the two cell types. However, during the invasion step (addition of Matrigel), cells distribute differently, with fibroblasts localized at the core of the spheroids, while TNBC cells leading the invasion into the Matrigel.

Supplementary Figure 3: Distribution of siRNA effects on MDA-MB-231 invasion.

Graphs depicting the Δ_{Ratio} siRNA screening values and distribution plots for different kinases in (**A**) HMF and (**B**) MRC5 cells. P-values were calculated using Student's t-test and were further processed using the Bonferroni correction method. Lower panels show a magnification of the graph for Kinases with Δ_{Ratio}<0.5. The overlapping hits (PIK3Cδ and AURKA) are highlighted in blue in both graphs.

Supplementary Figure 4: mRNA expression levels of PIK3Cδ in different cell lines/types and examination of TNBC expression of PIK3Cδ following co-culturing with fibroblasts.

(**A**) qRT-PCR of PIK3Cδ expression levels in BC, lymphoid and primary or immortalized fibroblast cell lines. (**B**) RNAseq data, courtesy of Human Protein Atlas (www.proteinatlas.org) showing the expression of PIK3Cδ in various lymphoid, myeloid, fibroblast and BC cell lines.(**C**) Western blotting of PIK3Cδ expression in MDA-MB-231 and BT-549 cells, following co-culturing with fibroblast cells (MRC5 or HMF) for a period of 9 days. GADPH was used as loading control. (**D**) Upper panel: Western blotting of PIK3Cδ expression in primary CAFs isolated from human TNBC samples. Lower panel: Effects of co-culturing CM isolated from primary CAFs on the expression of PIK3Cδ in BT-549 cells (for a period of 6 days). GADPH was used as loading control.

Supplementary Figure 5: Effects of silencing or overexpressing of fibroblast PIK3Cδ in TNBC invasion.

The effects of PIK3Cδ silencing in HMF (pool of 3 different siRNAs) on (**A**) MDA-MB-231 or (**B**) BT-549 invasion were assessed following the 3D experimental co-culture procedure described in Figure 1 (n=3 independent experiments, with at least 4 technical replicates). Significance was calculated using unpaired t-test. Results are expressed as mean ± SEM; * $p<0.05$, *** $P < 0.001$ vs control-siRNA transfected fibroblasts. (**C**) The knockdown efficacy of the PIK3Cδ siRNAs in HMF was verified by qRT-PCR. The effects of PIK3Cδ overexpression in HMF, using pCMV6-AC-PIK3Cδ-GFP plasmid, on (**D**) MDA-MB-231 or (**E**) BT-549 invasion were assessed following the same experimental procedure described in Figure 1 (n=3 independent experiments, with at least 4 technical replicates). Significance was calculated using unpaired t-test. Results are expressed as mean ± SEM; * $P < 0.05$ vs control-siRNA transfected fibroblasts. (**F**) The overexpression of PIK3Cδ in HMF was verified by qRT-PCR. (**G**) HMF and MRC5 cells were either transfected with pCMV6-AC-PIK3Cδ-GFP plasmid or silenced with PIK3Cδ siRNA for 24h and the CM from these treatments was collected. MDA-MB-231 were seeded in a 96 well plate (3000 cell/well), treated with the aforementioned CM for 48h and cell viability was assessed by CellTiter-Glo assay using a Glow-max reader (n=3 independent experiments, with 2 technical replicates). Significance was calculated using one-way ANOVA. Results are expressed as mean ± SEM.

Supplementary Figure 6: HT-RNAi screening validation.

(**A**) Genomic inhibition validation. Different shRNA plasmids targeting randomly selected kinases were used to transfect MRC5. 48h after transfection, fibroblasts were co-cultured with MDA-MB-231 cells and a 3D invasion assay was performed. Upper panel: Heatmap displaying the results of the shRNA inhibition compared to the original screening (siRNA) with regards to the invasion potential of MDA-MB-231. Lower panel: Representative pictures of the 3D invasion assay for certain kinases are shown. (**B**) qRT-PCR results demonstrating the silencing efficiency of the selected shRNAs plasmids against the respective kinases. (**C**) Pharmacological inhibition validation. MRC5 were pre-treated with 10 µM of the indicated compounds for 24h and then co-cultured in 3D with MDA-MB-231. Upper panel: Heatmap displaying the results of the chemical inhibition compared to the original screening (siRNA) with regards to the invasion potential of MDA-MB-231. Lower panel: Representative pictures of the 3D invasion assay for certain kinases are shown. (**D**) HMF and MRC5 cells were transfected with either siRNA or shRNA plasmids targeting PIK3Cδ or AURKA respectively and the cell viability was monitored 48h later using CellTiter-Glo assay. (n=3 independent experiments, with at least 2 technical replicates). Significance was calculated using two-way ANOVA. Results are expressed as mean ± SEM; ** $P < 0.01$, **** $P < 0.0001$ vs control transfected fibroblasts. (**E**) HMF and MRC5 cells were transfected with pCMV6-AC-PIK3Cδ-GFP plasmid and the cell viability was monitored 48h later using CellTiter-Glo assay. (n=3 independent

experiments, with at least 2 technical replicates). Significance was calculated using two-way ANOVA. Results are expressed as mean ± SEM.

Supplementary Figure 7: Effect of CAL-101 inhibitor on fibroblast cell lines.

(**A**) Western blotting of downstream targets of PIK3Cδ following treatment of HMF and MRC5 cells with increased concentrations of CAL-101. Each experiment was performed in triplicate. (**B**) HMF and MRC5 cells were treated with 5μM and 10μM of CAL-101 and the cell viability was monitored 48h later using CellTiter-Glo assay (n=3 independent experiments, with at least 4 technical replicates). Significance was calculated using two-way ANOVA test. Results are expressed as mean ± SEM; **** $P < 0.0001$ vs vehicle (DMSO) treated cells.

Supplementary Figure 8: Effects of chemical inhibition of PIK3Cδ on BT-549 cell invasion.

(A) 3D invasion assay: HMF (left panel) and MRC5 (right panel) were pre-treated with either vehicle (DMSO) or with 1, 5 and 10 μM of CAL-101 for 24h. Following, fibroblasts were co-cultured with BT-549 as 3D spheroids and the invasion potential was measured. Representative pictures of the 3D invasion assay at different time points are shown (n=3 independent experiments, with at least 4 technical replicates). Significance was calculated using unpaired t-test. Results are expressed as mean ± SEM; * $P < 0.05$ vs DMSO treated fibroblasts. (**B**) 2D invasion assay: HMF (left panel) and MRC5 (right panel) were pre-treated with either vehicle (DMSO) or with 1, 5 and 10 μM of CAL-101 for 24h and were then seeded on the lower chamber of a transwell insert. BT-549 cells were seeded on the Matrigel-coated upper chamber of the transwell insert (pore size: 8 μm allowing cell-crossing) and were co-cultured with the fibroblasts. After 24h of co-culture, migrated BT-549 cells were fixed and stained with crystal violet and counted using an inverted microscope (n=3 independent experiments, with at least 6 technical replicates). Significance was calculated using one-way ANOVA test. Data are expressed as mean ± SEM; ** $P < 0.01$, **** $P < 0.0001$ vs DMSO treated fibroblasts. (**C**) 2D real-time invasion assay: HMF (left panel) and MRC5 (right panel) were pre-treated with either vehicle (DMSO) or with 10 μM of CAL-101 for 24h and were then seeded on the lower chamber of a transwell insert. BT-549 cells were seeded on the upper chamber of the transwell insert (pore size: 0.4 μm not allowing cell-crossing) and were co-cultured with the fibroblasts. After 24h of co-culture, BT-549 were moved to CIM-Plates and their relative invasion rate was monitored using the xCELLigence Real-Time Cell Analysis (RTCA) instrument (n=3 independent experiments). Significance was calculated using two-way Anova test. Results are expressed as mean ± SEM; *** $P < 0.001$, **** $P < 0.0001$ vs DMSO treated fibroblasts. **(D)** 2D CM invasion assay: HMF (left panel) and MRC5 (right panel) were treated with vehicle only or with 10 μM CAL101 in serum free for 24h in order to obtain the CM. BT-549 were then incubated with HMF or MRC5 CM for 2D invasion

assays (n=3 independent experiments). Significance was calculated using unpaired t-test. Data are expressed as mean ± SEM; * P < 0.05, ** P < 0.01 vs DMSO treated fibroblasts' CM. (**E**) 2D invasion assay: TNBC patients' CAFs were pre-treated with either vehicle (DMSO) or with 10 µM of CAL-101 for 24h and were then seeded on the lower chamber of a transwell insert. BT-549 cells were seeded on the Matrigel-coated upper chamber of the transwell insert (pore size: 8 µm allowing cell-crossing) and were co-cultured with the TNBC CAFs. After 24h of co-culture, migrated BT-549 cells were fixed and stained with crystal violet and counted using an inverted microscope. (*n*=3 independent experiments, with at least 4 technical replicates). Significance was calculated using unpaired t-test. Data are expressed as mean ± SEM; **** P < 0.0001 vs DMSO treated fibroblasts.

Supplementary Figure 9:

2D invasion assay: TNBC patients' CAFs were pre-treated with either DMSO or with 10 µM of CAL-101 for 24h and were then seeded on the lower chamber of a transwell insert. MDA-MB-231 cells were seeded on the Matrigel-coated upper chamber of the transwell insert and were co-cultured with the TNBC CAFs. 24h after co-culture, migrated MDA-MB-231 cells were fixed, stained with crystal violet and counted using an inverted microscope (n=2 independent experiments, with at least 5 technical replicates). Significance was calculated using unpaired t-test. Data are expressed as mean ± SEM; **** P< 0.0001 vs DMSO treated fibroblasts.

Supplementary Figure 10: Recovery of PIK3Cδ mRNA levels after silencing with shRNA or siRNA.

(**A**) MRC5 were transfected with control or PIK3Cδ siRNA (left panel) or control or PIK3Cδ shRNA (right panel). Silenced MRC5 were transfected 24h later with the pCMV6-AC-PIK3Cδ-GFP plasmid. PIK3Cδ expression levels were monitored during the course of the experiment. Significance was calculated using one-way ANOVA, followed by Dunnett's testunpaired t-tests.. Results are expressed as mean ± SEM; ** P < 0.01, ***P < 0.001 vs PIK3Cδ silenced or vs. PIK3Cδ overexpressed cells. (**B**) MRC5 were transfected with control or PIK3Cδ siRNA (left panel) or control or PIK3Cδ shRNA (right panel). MDA-MB-231 cells were incubated with MRC5 cells and 2D invasion assays were performed. Silenced MRC5 were transfected with either pCMV6-AC-GFP vector or with pCMV6-AC-PIK3Cδ-GFP plasmid. MDA-MB-231 cells were then incubated with MRC5 cells and 2D invasion assays were performed (n=2 independent experiments, with at least 5 technical replicates). Significance was calculated using one-way Anova and Tukey's multiple comparisons tests. Data are expressed as mean ± SEM; ** P < 0.01 ****P < 0.0001 vs samples indicated in the graph.

Supplementary Figure 11: Effects of various PI3K inhibitors on TNBC cell invasion and fibroblasts' cell viability.

(A) Table showing the selectivity of specific inhibitors against different PI3K isoforms. **(B)** 2D invasion assay: MRC5 and HMF cells were pre-treated with either vehicle (DMSO) or with different concentrations of various PIK3 inhibitors for 24h and were then seeded on the lower chamber of a transwell insert. MDA-MB-231 and BT-549 cells were seeded on the Matrigel-coated upper chamber of the transwell insert (pore size: 8 μm allowing cell-crossing) and were co-cultured with the fibroblasts. After 24h of co-culture, migrated MDA-MB-231 cells were fixed and stained with crystal violet and counted using an inverted microscope (n=2 independent experiments, with at least 5 technical replicates). Significance was calculated using one-way ANOVA test. Data are expressed as mean ± SEM; * $P < 0.05$, *** $P < 0.001$, **** $P < 0.0001$ vs DMSO treated fibroblasts. **(C)** MRC5 cells and HMF were treated with different concentrations of various PIK3 inhibitors and the cell viability was monitored 48h later using CellTiter-Glo assay. (n=2 independent experiments, with at least 2 technical replicates) Significance was calculated using two-way ANOVA test. Results are expressed as mean ± SEM.

Supplementary Figure 12: Principal component analysis (PCA) plot and cluster analysis of RNA-seq samples. (**A**) PCA performed using DESeq2 rLog-normalized RNAseq data. Loadings for principal components 1 (PC1) and PC2 are reported in the graph. (**B**) Hierarchical clustering analyses performed using DESeq2 rLog-normalized RNAseq data. Color code from white to dark blue refers to the distance metric used for clustering, with dark blue referring to maximum of correlation values.

Supplementary Figure 13: Fibroblast-PIK3Cδ / cancer epithelial cells-NR4A1 paracrine signaling axis promotes TNBC invasion.

(**A**) Western blotting of NR4A1 expression in a panel of BC cell lines. GADPH was used as loading control. (**B**) 2D invasion assay: BT-549 cells were seeded on the Matrigel-coated upper chamber of the transwell insert (pore size: 8 μm allowing cell-crossing) and were treated with either vehicle (DMSO) or Cytosporone B (5 μM). After 24h, migrated BT-549 cells were fixed and stained with crystal violet and counted using an inverted microscope (n=3 independent experiments, with at least 4 technical replicates). Significance was calculated using unpaired t-test. Results are expressed as mean ± SEM; **** $P < 0.0001$ vs DMSO treated cells. (**C**) HMF cells were treated with CAL-101 or DMSO. NR4A1-silenced (siRNA) MDA-MB-231 or control-siRNA cells were seeded on the Matrigel-coated upper chamber of a transwell insert (pore size: 8 μm allowing cell-crossing) and were co-cultured with fibroblasts. After 24h of co-culture, migrated MDA-MB-231 cells were fixed and stained with crystal violet and counted using an inverted microscope. (n=3 independent experiments,

with at least 3 technical replicates). Significance was calculated using two-way ANOVA test. Results are expressed as mean ± SEM; ** P < 0.01, ***P<0.001, **** P < 0.0001 vs samples indicated in the graph. (**D**) qRT-PCR of NR4A1 expression levels in MDA-MB-231 cells transfected with the respective siRNAs. (**E**) Western blotting of NR4A1 expression levels in MDA-MB-231 cells transfected with the respective siRNAs. α-Tubulin was used as loading control. (**F**) NR4A1-silenced (siRNA) MDA-MB-231 or control-siRNA cells were analyzed for NR4A1, NR4A2 and NR4A3 mRNA expression by qRT-PCR. (**G**) NR4A1-silenced (siRNA) MDA-MB-231 or control-siRNA cells were seeded on the Matrigel-coated upper chamber of a transwell insert (pore size: 8 μm allowing cell-crossing) and were treated with either vehicle (DMSO) or Cytosporone B (5 μM). After 24h, migrated MDA-MB-231 cells were fixed and stained with crystal violet and counted using an inverted microscope. (n=3 independent experiments, with at least 3 technical replicates). Significance was calculated using two-way ANOVA test. Results are expressed as mean ± SEM; ** P < 0.01, **** P < 0.0001 vs control.

Supplementary Figure 14: Schematic of integrated secretome and RNAseq analysis.

Supplementary Figure 15: *In silico* prediction of secreted proteins altering NR4A1-mediated invasion of TNBC cells.

Custom pathway built using the IPA showing how secreted proteins from CAL-101 treated MRC5 cells may regulate cell invasion of MDA-MB-231 cells via upregulation of NR4A1 pathway. The red and green color of the secreted factors indicates increased and decreased expression respectively while the red arrow signifies activation.

Supplementary Figure 16: Effects of BDNF or PLGF treatment on NR4A1 expression and invasion of BT-549 cells.

(**A**) qRT-PCR of *NR4A1* expression levels in BT-549 cells following treatment with PLGF and BDNF (or control PBS/BSA (0.1%)). (**B**) 2D invasion assay: BT-549 cells were seeded on the Matrigel-coated upper chamber of the transwell insert (pore size: 8 μm allowing cell-crossing) and were treated with PLGF or BDNF (or control PBS/BSA (0.1%)). After 24h, migrated BT-549 cells were fixed and stained with crystal violet and counted using an inverted microscope (n=3 independent experiments, with at least 4 technical replicates). Significance was calculated using unpaired t-test. Results are expressed as mean ± SEM; ** P < 0.01, *** P < 0.001, **** P < 0.0001 vs vehicle treated cells.

Supplementary Figure 17: Effects of BDNF or PLGF silencing on CAL-101 mediated TNBC cell invasion.

(**A**) MRC5 cells transfected with siRNA for BDNF and/or PLGF were pre-treated with either vehicle (DMSO) or 10 µM of CAL-101 for 24h. MDA-MB-231 cells were seeded on the Matrigel-coated upper chamber of a transwell insert (pore size: 8 µm allowing cell-crossing) and were co-cultured with the fibroblasts. After 24h of co-culture, migrated MDA-MB-231 cells were fixed, stained with crystal violet and counted using an inverted microscope (n=3 independent experiments, with at least 3 technical replicates). Significance was calculated using two-way ANOVA test. Results are expressed as mean ± SEM; * $P < 0.01$ vs DMSO treated control cells. (**B**) qRT-PCR of BDNF and PLGF expression levels in fibroblasts transfected with the respective siRNAs.

Supplementary Figure 18: Effects of CAL-101 treatment on MDA-MB-231 cell viability.
MDA-MB-231 cells were treated with either vehicle (DMSO) or increasing concentrations of CAL-101 and cell viability was monitored after 24h, 48h and 72h using CellTiter-Glo assay. (n=3 independent experiments, with at least 5 technical replicates). Significance was calculated using two-way ANOVA test. Results are expressed as mean ± SEM; * $P < 0.05$, ** $P < 0.01$ vs vehicle treated cells.

Supplementary Figure 19: Expression of $CD68^+$ cells in the immunocompromised orthotopic BC xenograft model.
Representative images of immunofluorescent staining of MDA-MB-231/MRC5 tumor cryosections for CD68 (red) and p-AKT (Thr308) (green) after vehicle or CAL-101 treatment. Original magnification, 40x. Scale bar, 50µm. The quantification of p-AKT (Thr308) immunofluorescent staining in tumor infiltrating CD68 macrophages were very low (white arrows) without difference between the groups. Statistics were not performed.

Supplementary Figure 20: Effects of CAL-101 treatment on tumor growth of MMTV-PyMT transgenic mice.
(**A**) Tumor volumes chart from MMTV-PyMT transgenic mice after vehicle or CAL-101 treatment Individual values for each mouse are displayed. Significance was calculated using unpaired t-test (week 15). Results are expressed as mean ± SEM; * $P < 0.05$. **(B)** Images of tumors, lungs and livers of MMTV-PyMT transgenic mice after vehicle or CAL-101 treatment are shown. Yellow arrows indicate gross appearance of metastatic lung tumor nodes in different mice from both treatment groups. **(C)** Representative images of lung tissues and hematoxylin and eosin staining from MMTV-PyMT mice that were treated with either vehicle or CAL-101. (Scale bar, 5mm). **(D)** Upper panel: Representative images of immunofluorescent staining for α-SMA and total PIK3Cδ in the mammary tumor sections of MMTV-PyMT transgenic mice after vehicle or CAL-101 treatment. Arrows indicate a-SMA^+ fibroblasts. Higher-magnification images are shown at the bottom right corner.

Lower panel: Quantification of p- total PIK3Cδ immunofluorescent staining in tumor infiltrating a-SMA$^+$ fibroblasts in the mammary tumors of MMTV-PyMT transgenic mice after vehicle or CAL-101 treatment. Significance was calculated using multiple t-tests. Results are expressed as mean ± SEM. **(E)** Upper panel: Representative images of immunofluorescent staining for F4/80 and total PIK3Cδ in the mammary tumor sections of MMTV-PyMT transgenic mice after vehicle or CAL-101 treatment. Arrows indicate F4/80$^+$ macrophages. Higher-magnification images are shown at the bottom right corner. Lower panel: Quantification of total PIK3Cδ immunofluorescent staining in tumor infiltrating F4/80$^+$ macrophages in the mammary tumors of MMTV-PyMT transgenic mice after vehicle or CAL-101 treatment. Significance was calculated using multiple t-tests. Results are expressed as mean ± SEM. (**F**) Western blotting of PIK3Cδ expression in CAFs and cancer cells isolated MMTV-PyMT tumors. The expression of PIK3Cδ expression following co-culturing with CM isolated from CAFs for a period of 6 days was also examined. GADPH was used as loading control.

Supplementary Figure 21: BDNF, PLGF and NR4A1 expression in MMTV-PyMT tumors.
Representative images of IHC staining of the mammary tumor sections of MMTV-PyMT transgenic mice stained for BDNF, PLGF and NR4A1, after vehicle or CAL-101 treatment. Significance was calculated using unpaired t-test. Results are expressed as mean ± SEM; * $P < 0.05$, *** $P < 0.001$ vs vehicle treated tumors. Original magnification, 20×. The intensity of BDNF, PLGF and NR4A1 signals were evaluated in the vehicle treated tumor slides and then this value was compared with the signals from CAL-101 treated tumor slides results are expressed as percentage of signal vs vehicle treated tumors.

Supplementary Figure 22: PIK3Cδ expression in tumor and fibroblast cells.
Representative images of low and high PIK3Cδ expression in tumor or surrounding fibroblast cells (a-SMA+) are shown. **(A)** Low PIK3Cδ expression in tumoural and intra- tumoural fibroblasts. **(B)** α-SMA positive expression in same field for quantifying PIK3Cδ expression in intra- tumoral fibroblasts. **(C)** High PIK3Cδ expression in tumoral and intra- tumoral fibroblasts. **(D)** α-SMA positive expression in same field for quantifying PIK3Cδ expression in intra- tumoral fibroblasts. Original magnifications: ×2, x5, 10x. Scale bars: 200, 500, 1000 μm. The red arrows represent the fibroblast expression of PIK3Cδ, while the black arrows represent the tumoral expression of PIK3Cδ.

Supplementary Figure 23: Association of tumoral-PIK3Cδ expression with patients' survival.
(**A**) Kaplan-Meier plots showing the association between tumoral-PIK3Cδ protein expression with OS ($P = 0.004$) in TNBC patients. (**B**) Kaplan-Meier plots showing the association between tumoral-

PIK3Cδ protein expression with DFS (P = 0.009) in TNBC patients. (**C**) Kaplan-Meier plots showing the association between tumoral-PIK3Cδ mRNA expression with OS (P = 0.405) in TNBC patients following deconvolution of bulk TCGA RNA-seq samples. (**D**) Kaplan-Meier plots showing the association between CAF-PIK3Cα mRNA expression with OS (P = 0.014) in TNBC patients following deconvolution of bulk TCGA RNA-seq samples. (**E**) Kaplan-Meier plots showing the association between CAF-PIK3Cβ mRNA expression with OS (P = 0.0123) in TNBC patients following deconvolution of bulk TCGA RNA-seq samples. (**F**) Kaplan-Meier plots showing the association between CAF-PIK3Cγ mRNA expression with OS (P = 0.493) in TNBC patients following deconvolution of bulk TCGA RNA-seq samples. * $P < 0.05$, ** $P < 0.01$.

Supplementary Figure 1

A

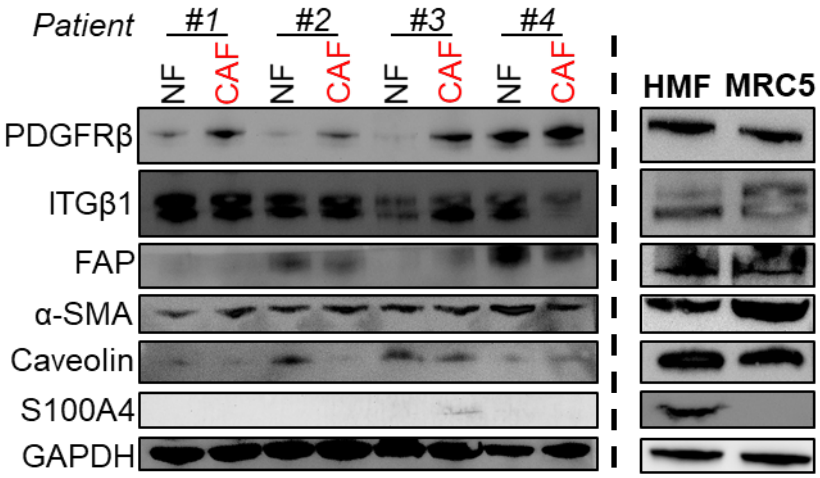

B

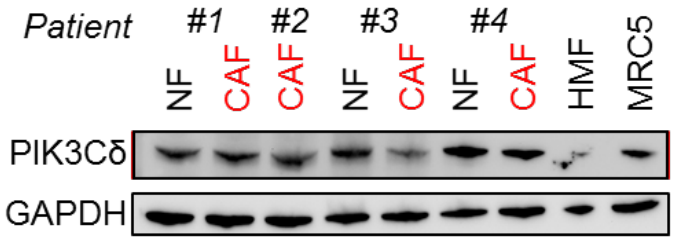

C

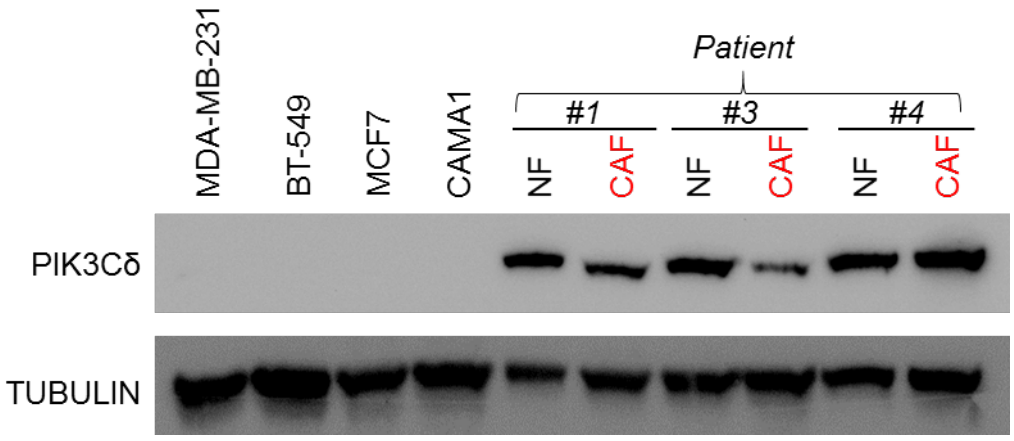

Supplementary Figure 2

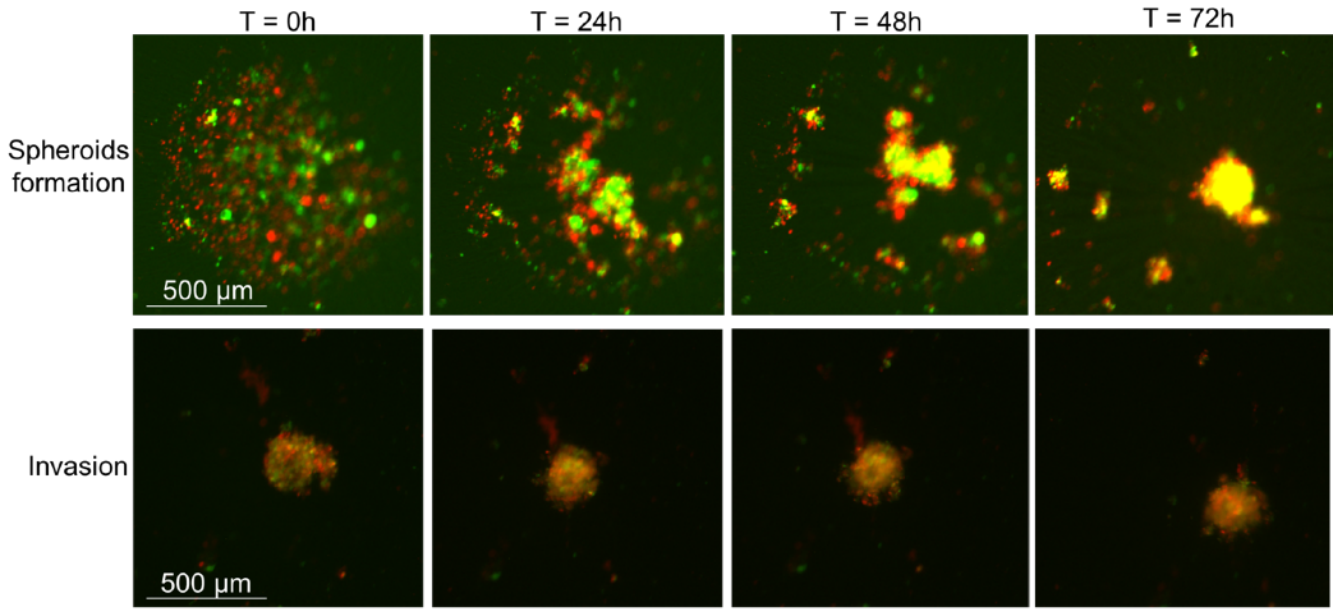

Supplementary Figure 3

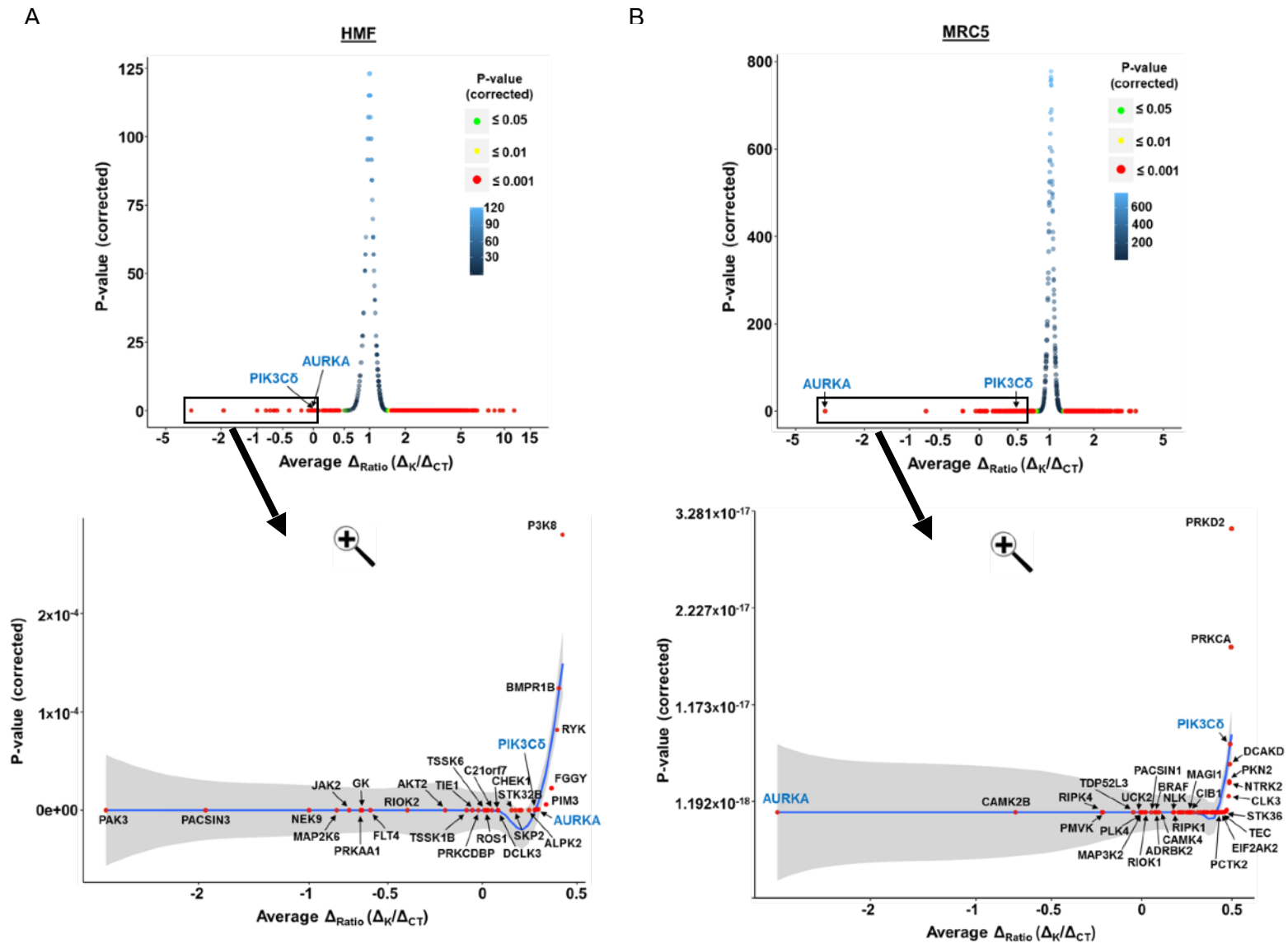

Supplementary Figure 4

A

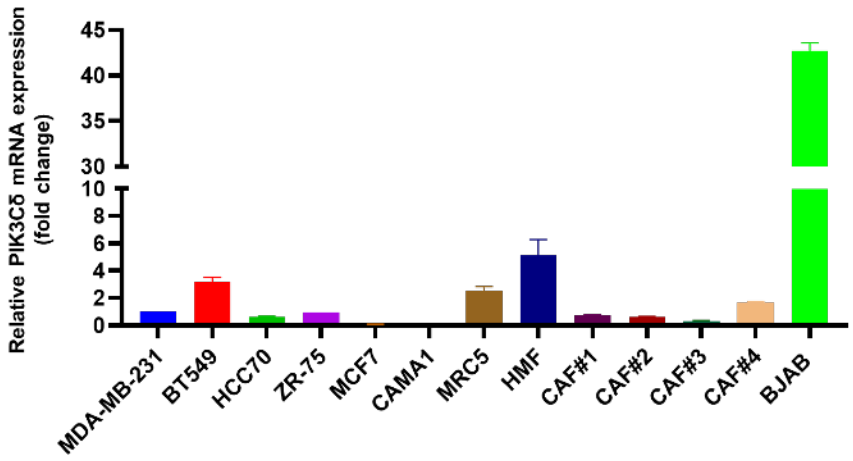

B

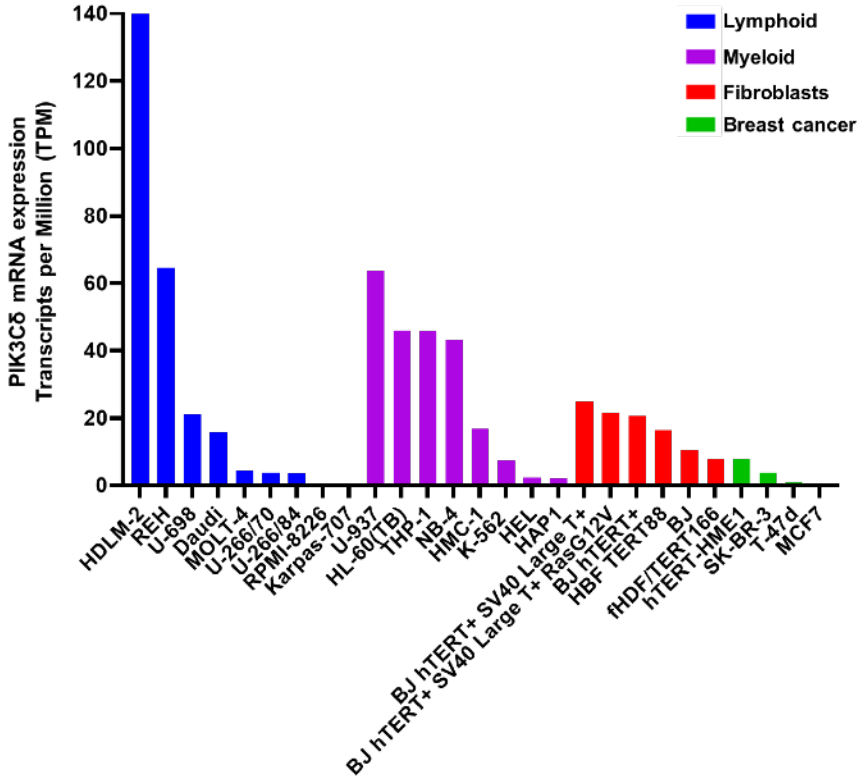

C

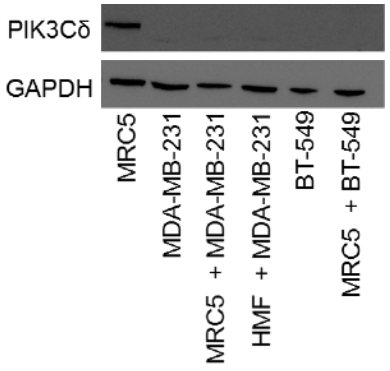

D

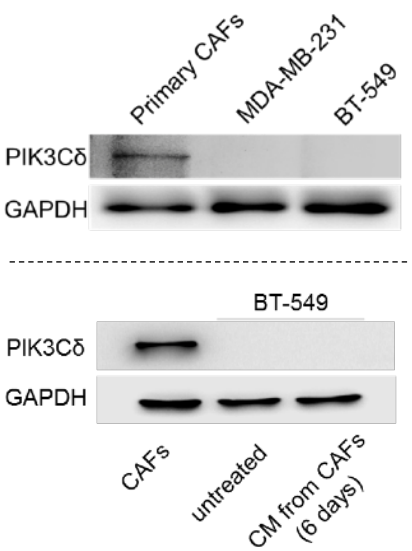

Supplementary Figure 5

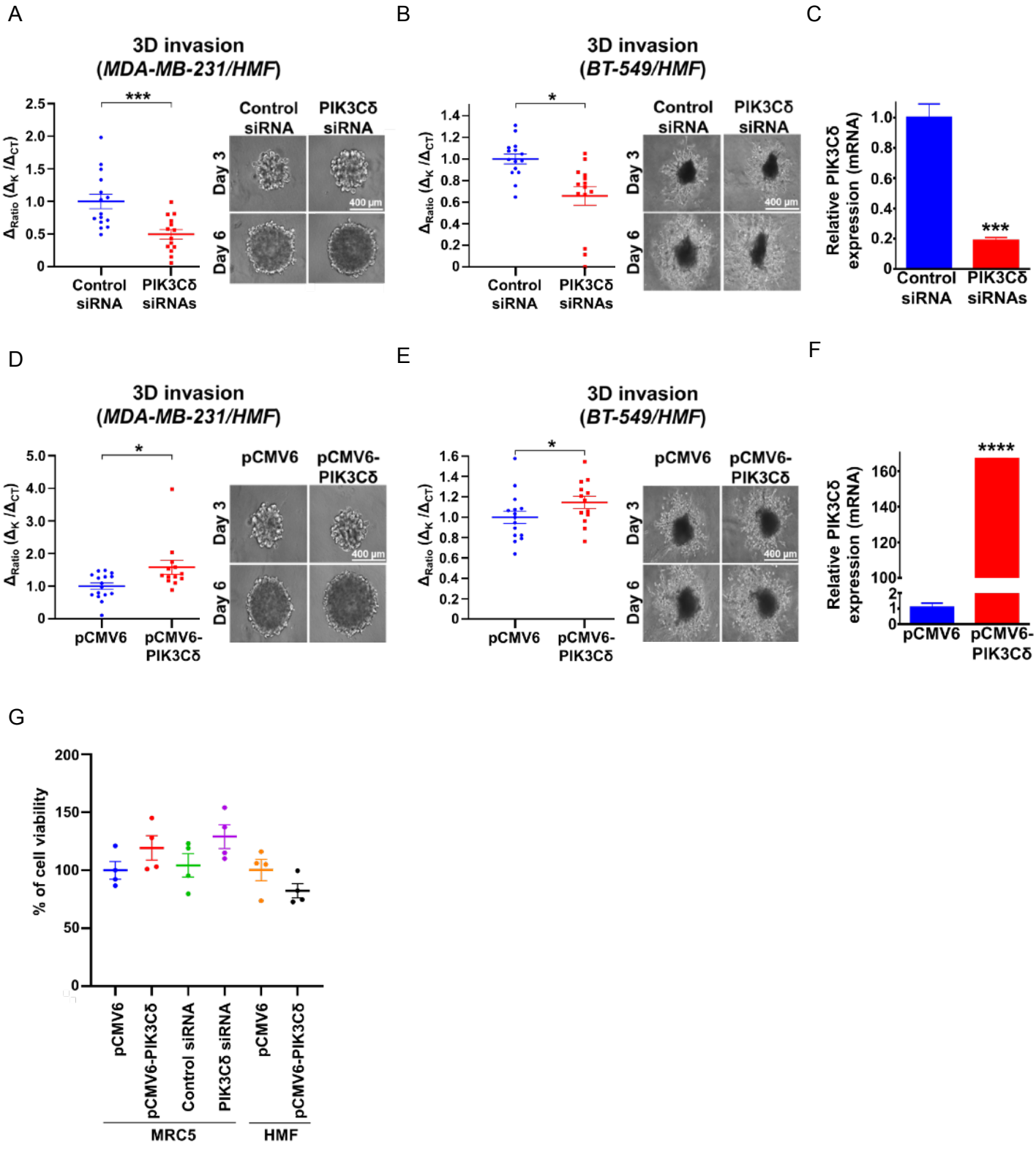

Supplementary Figure 6

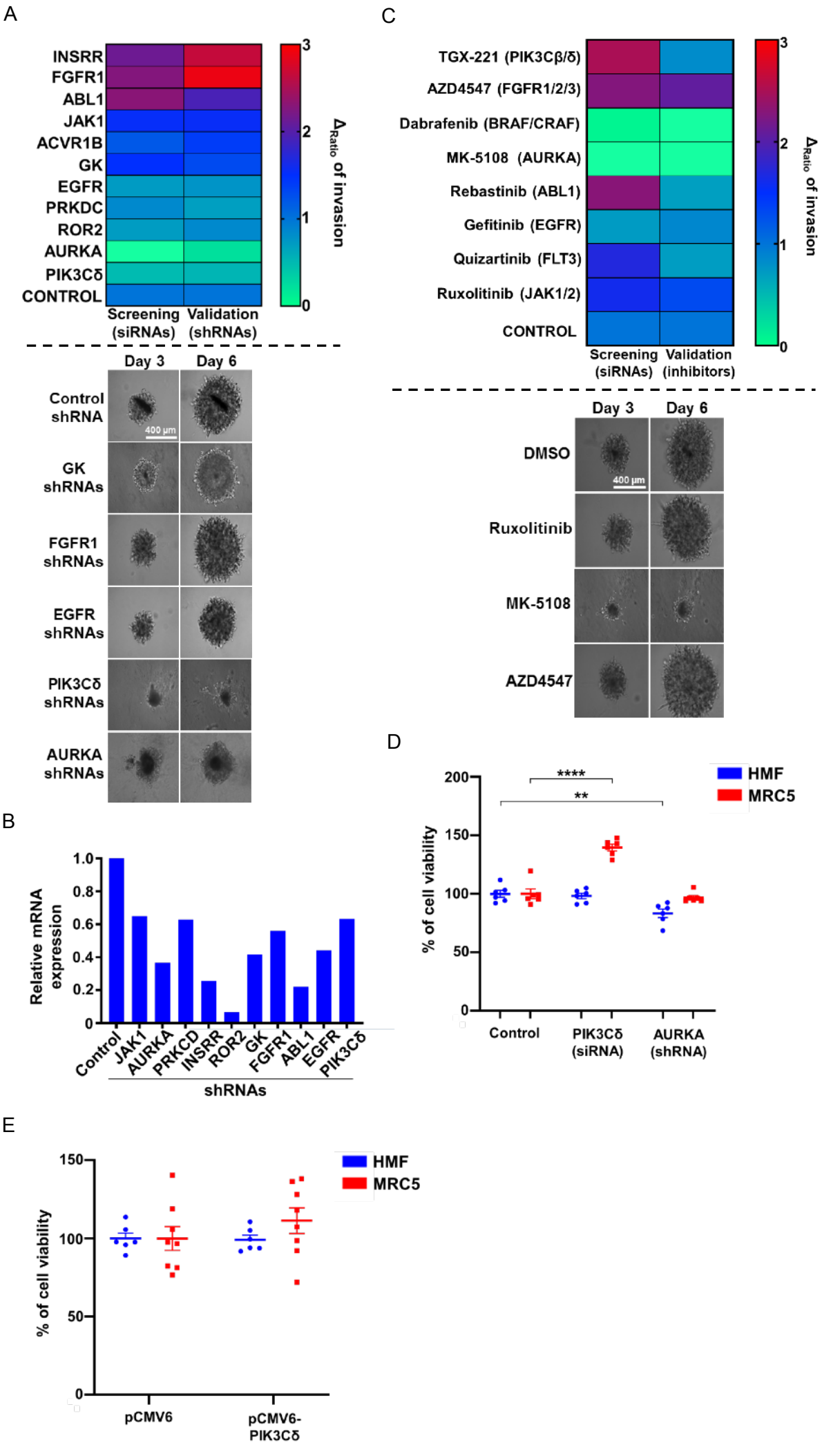

Supplementary Figure 7

A

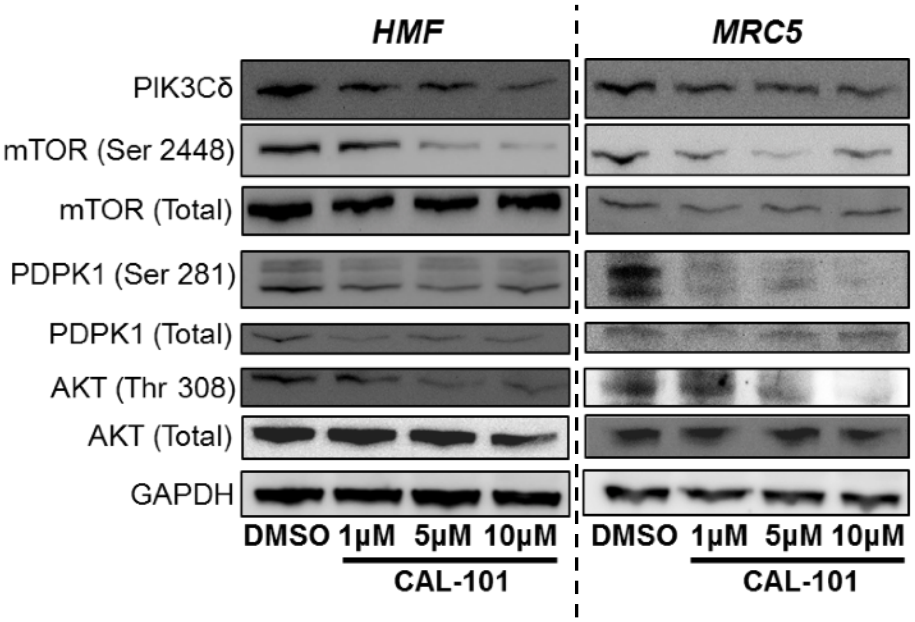

B

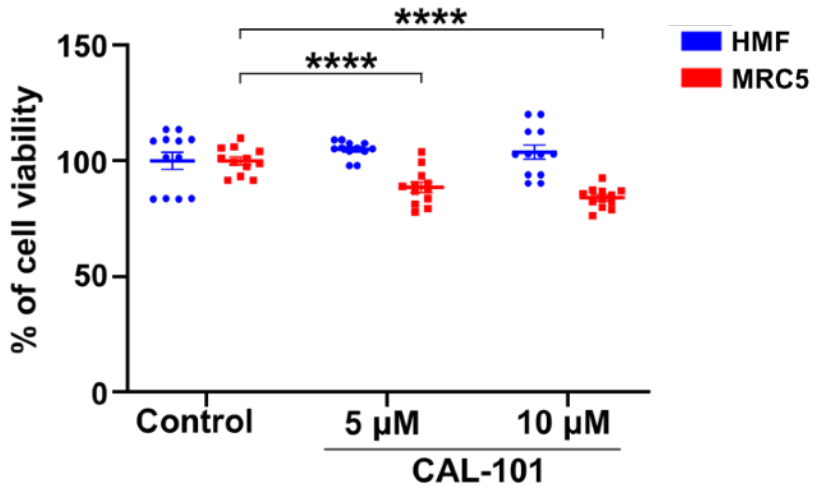

Supplementary Figure 8

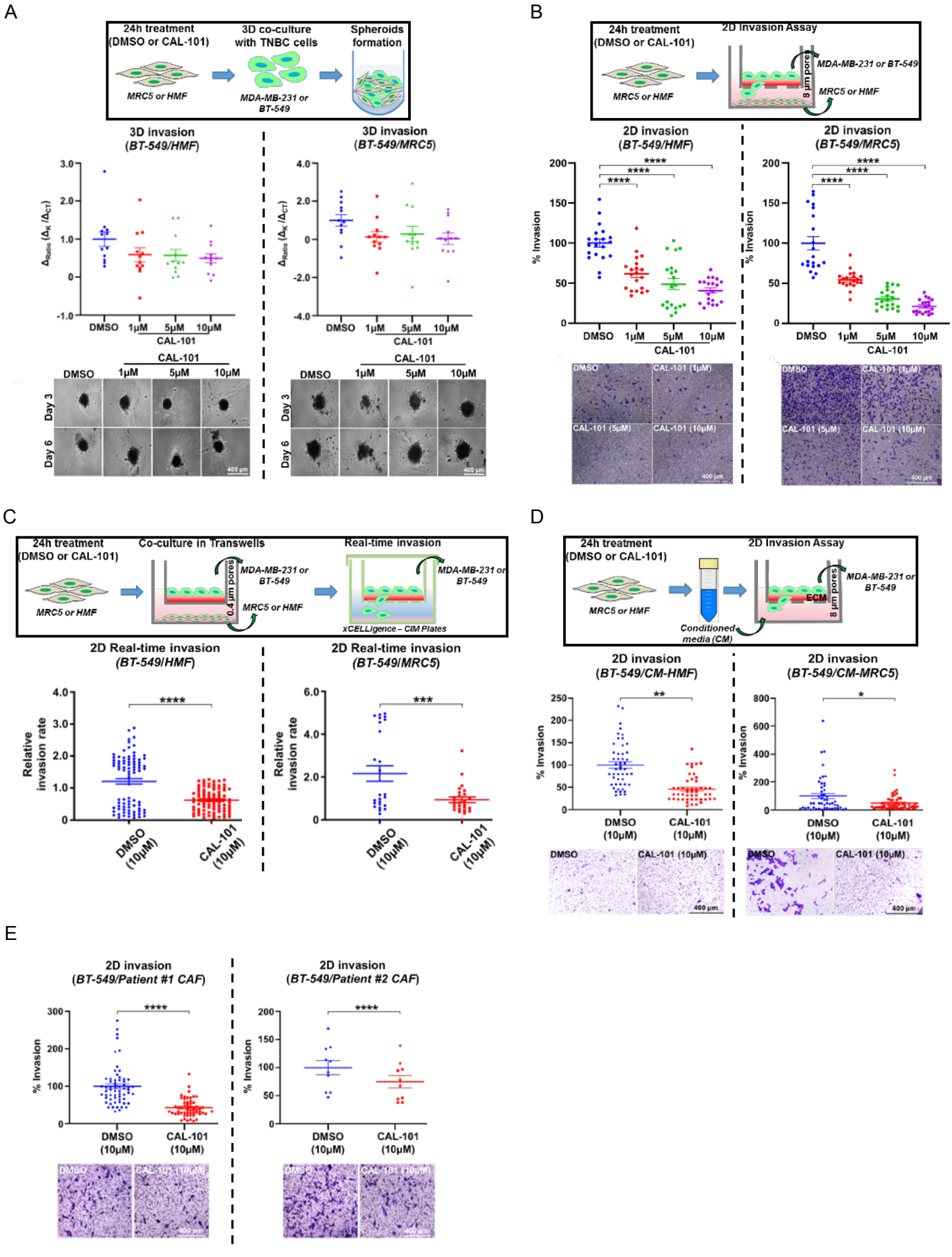

Supplementary Figure 9

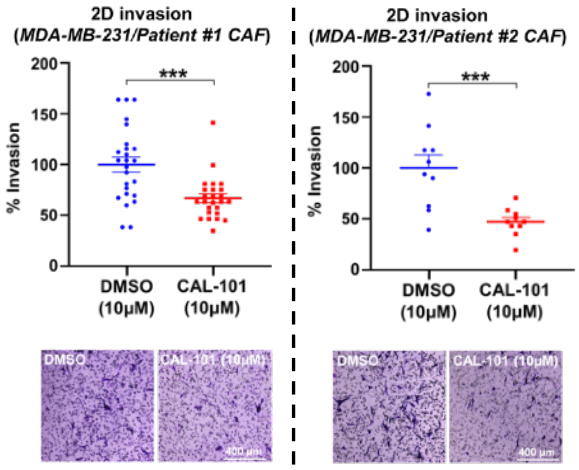

Supplementary Figure 10

A

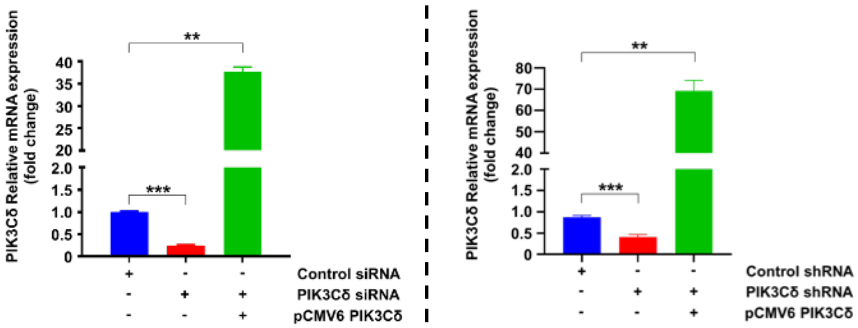

B

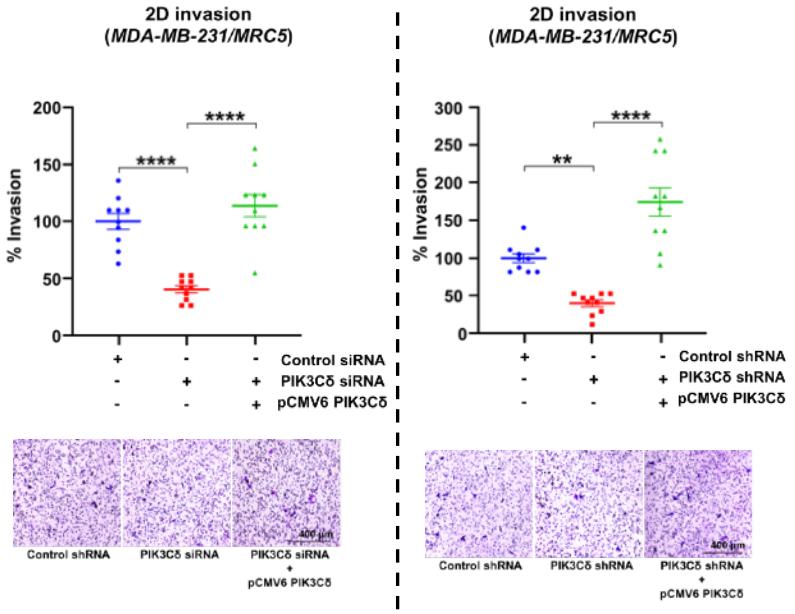

Supplementary Figure 11

A

PIK3C isoform	PIK3 inhibitor				
	AS252424	PI-103	CAL-101	Leniolisib (CDZ 173)	NVP-BEZ235
α	+	++++		+	++++
β		++++		+	++
γ	++	+++	++	+	++++
δ		++++	++++	++++	+++

B

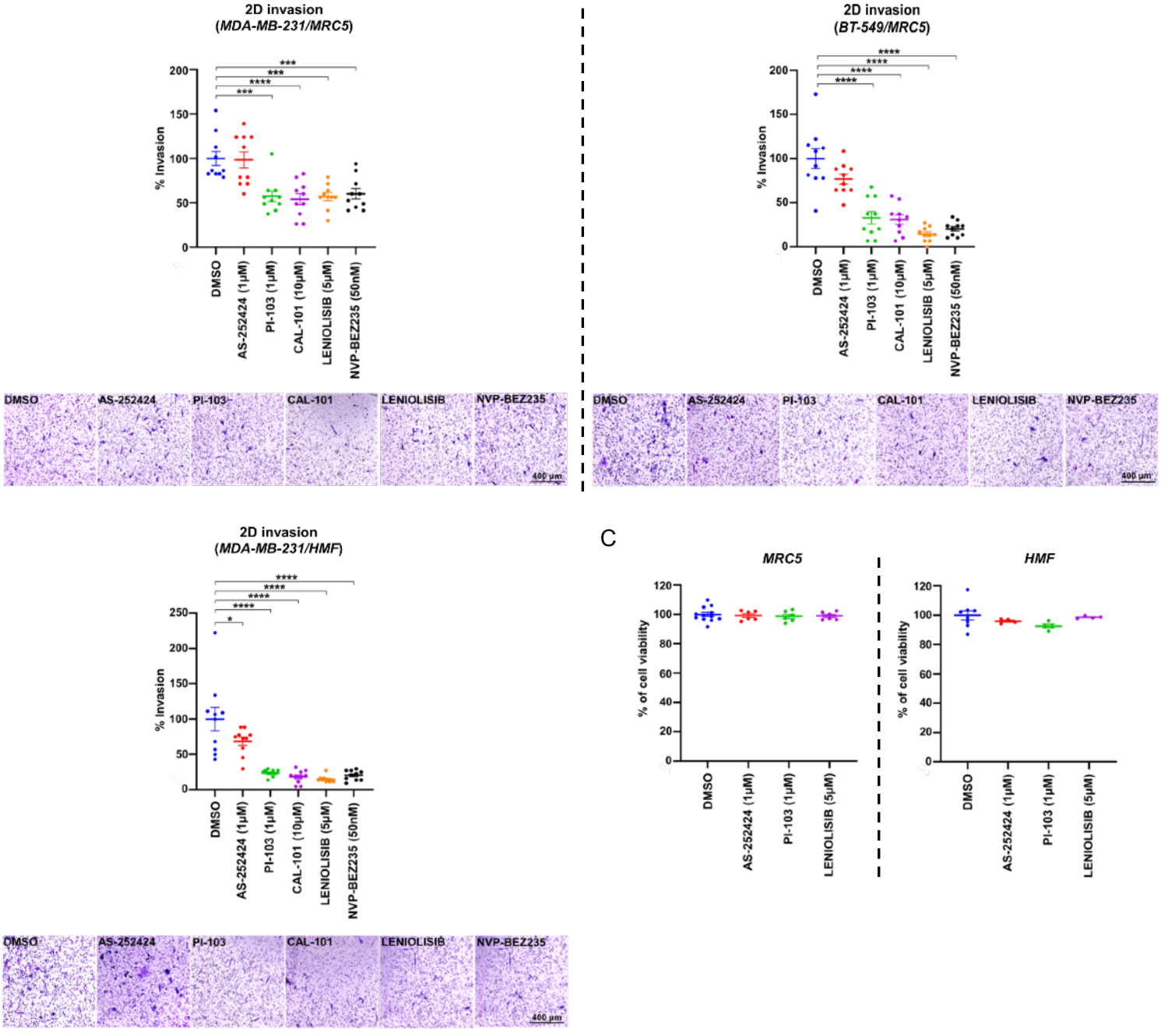

C

Supplementary Figure 12

A

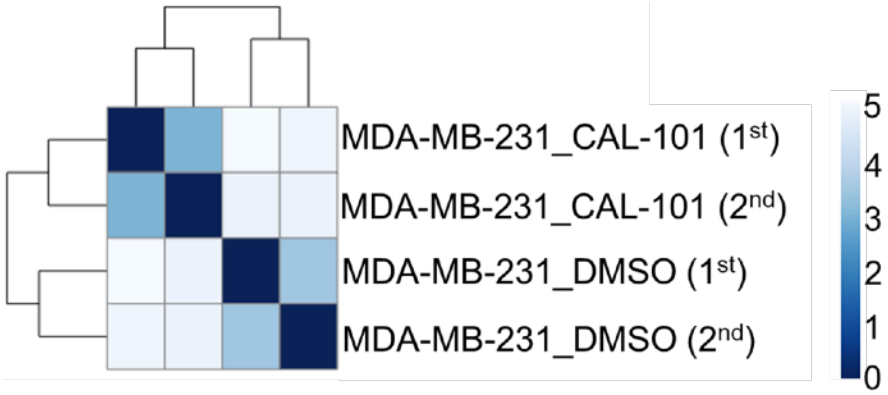

B

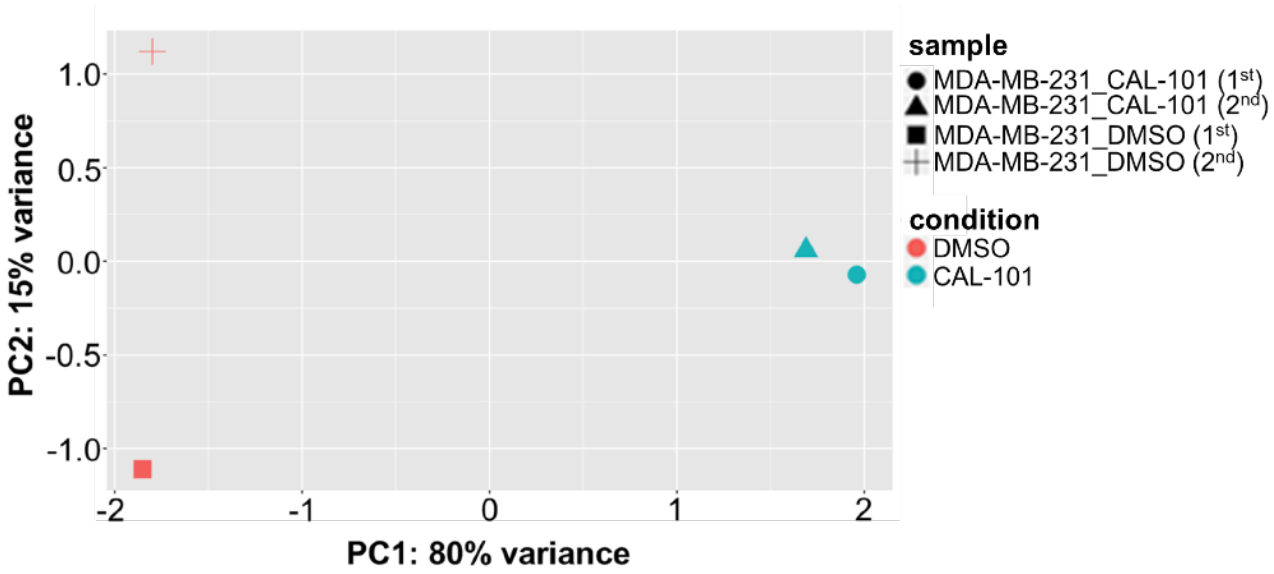

Supplementary Figure 13

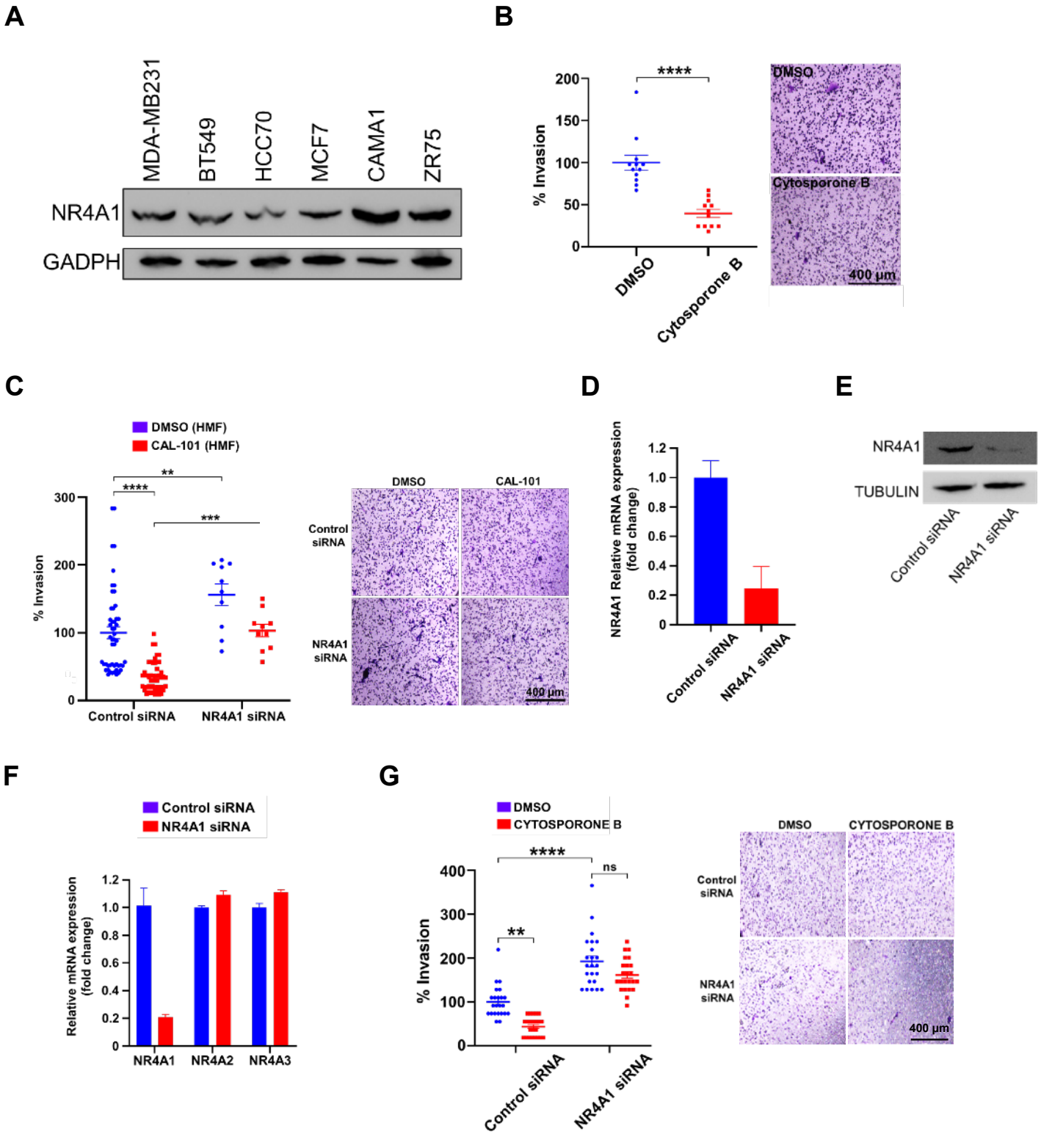

Supplementary Figure 14

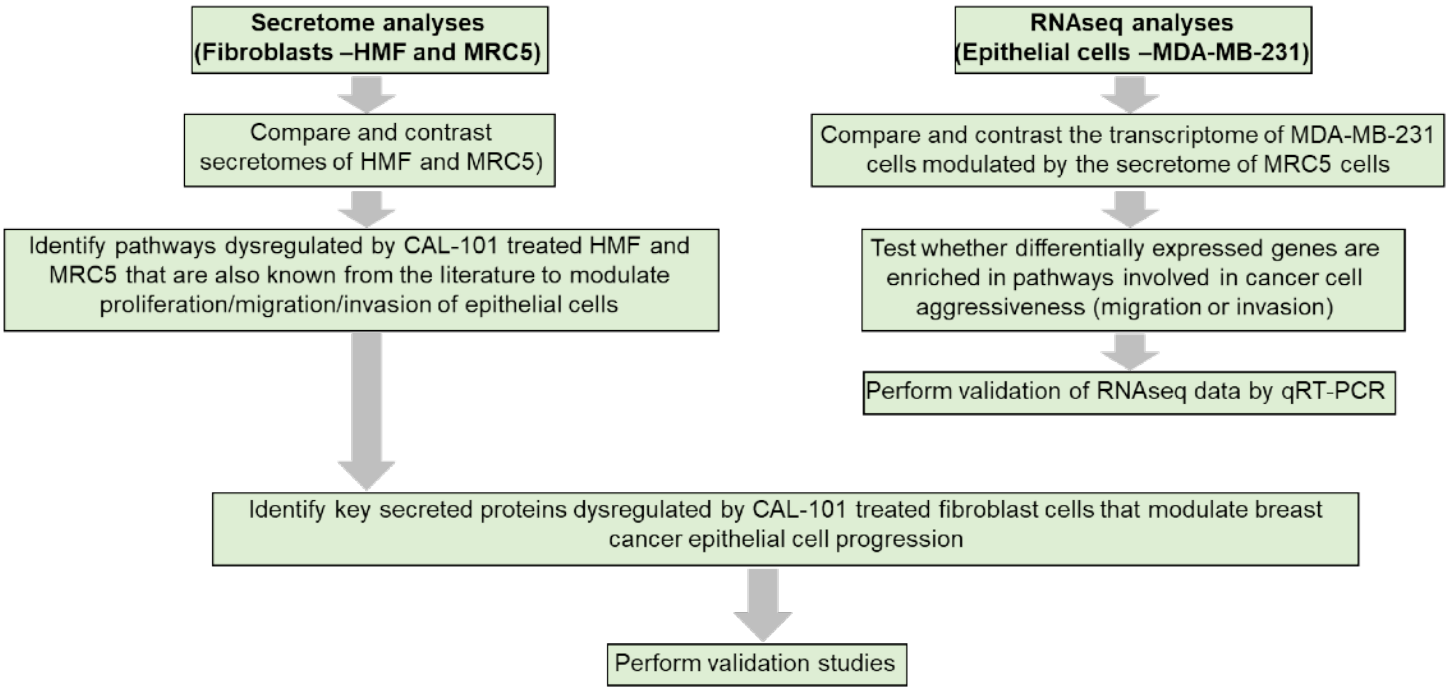

Supplementary Figure 15

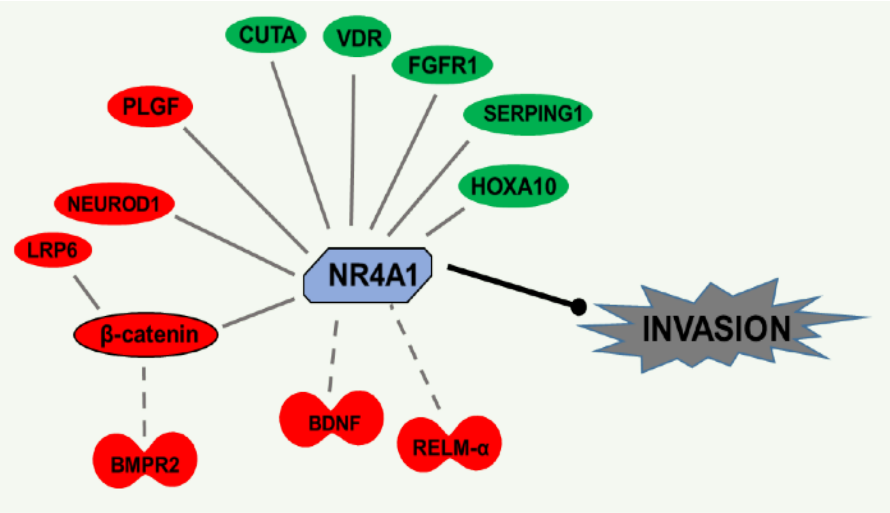

Supplementary Figure 16

A

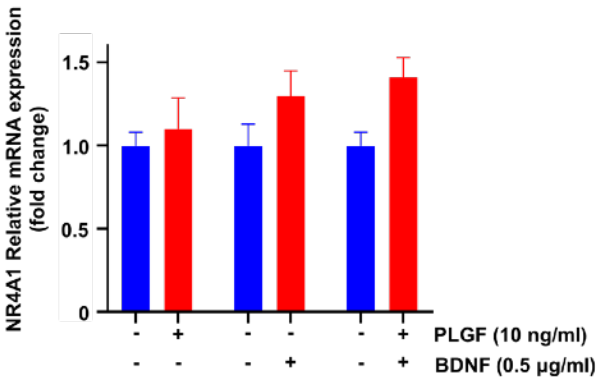

B

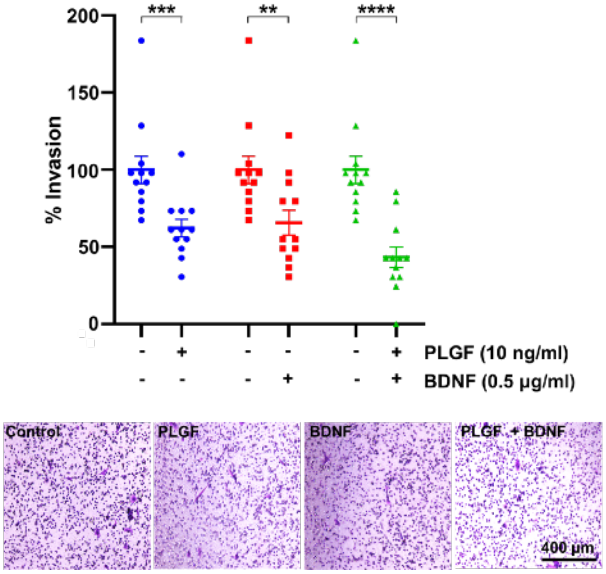

Supplementary Figure 17

A

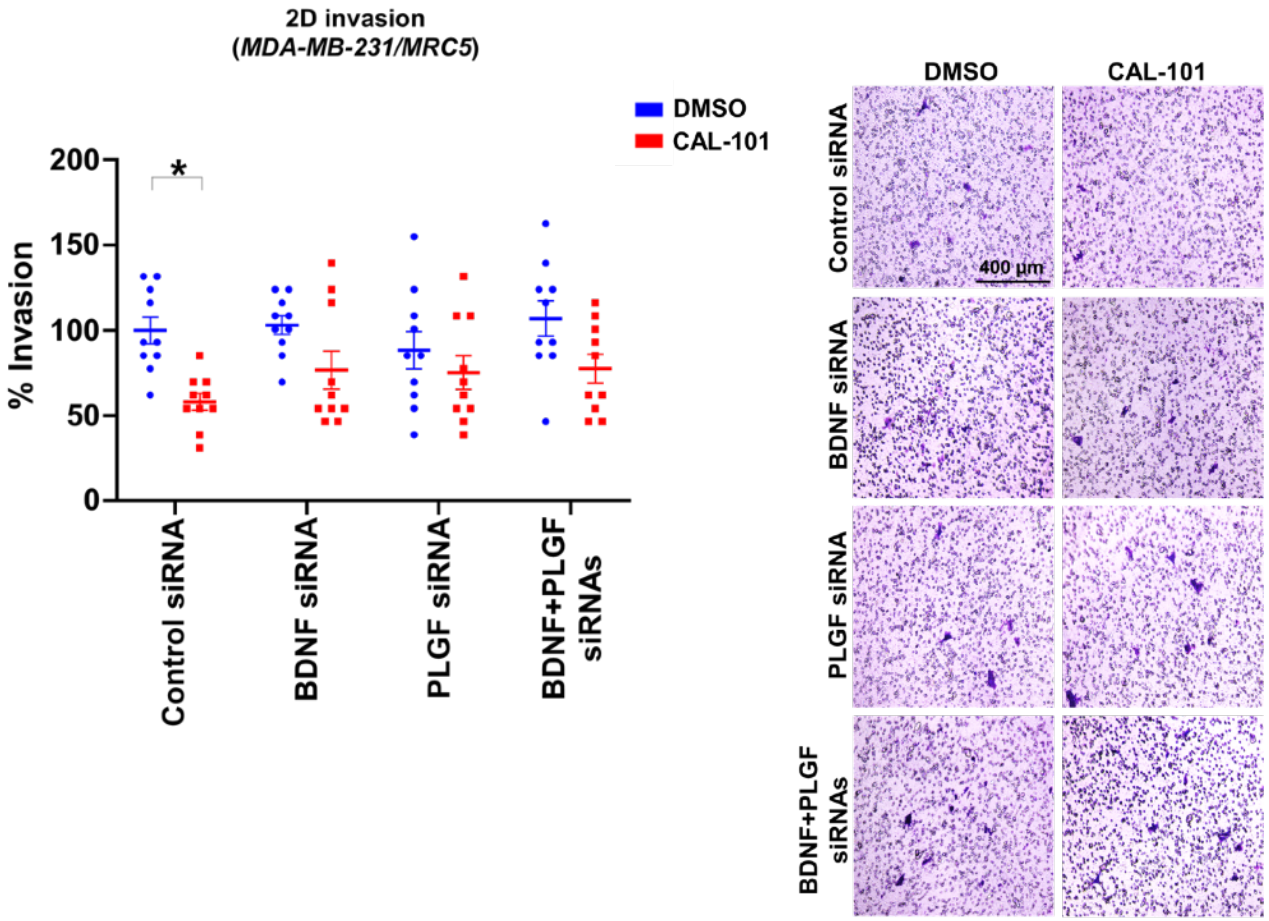

B

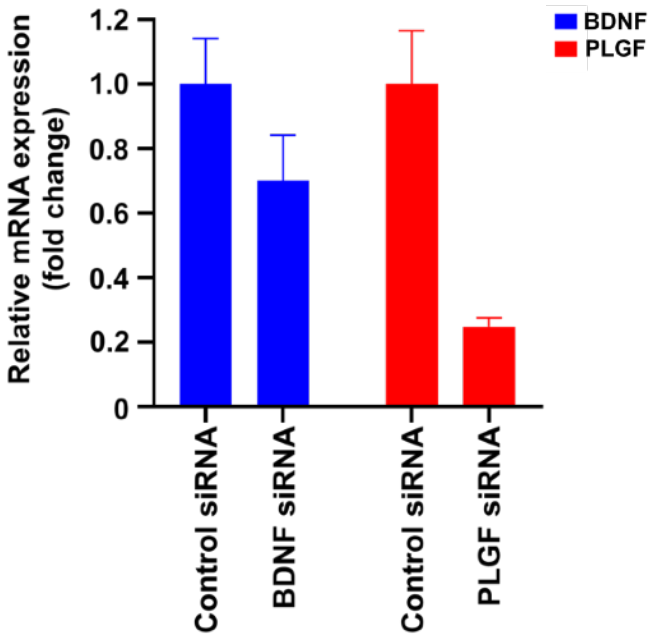

Supplementary Figure 18

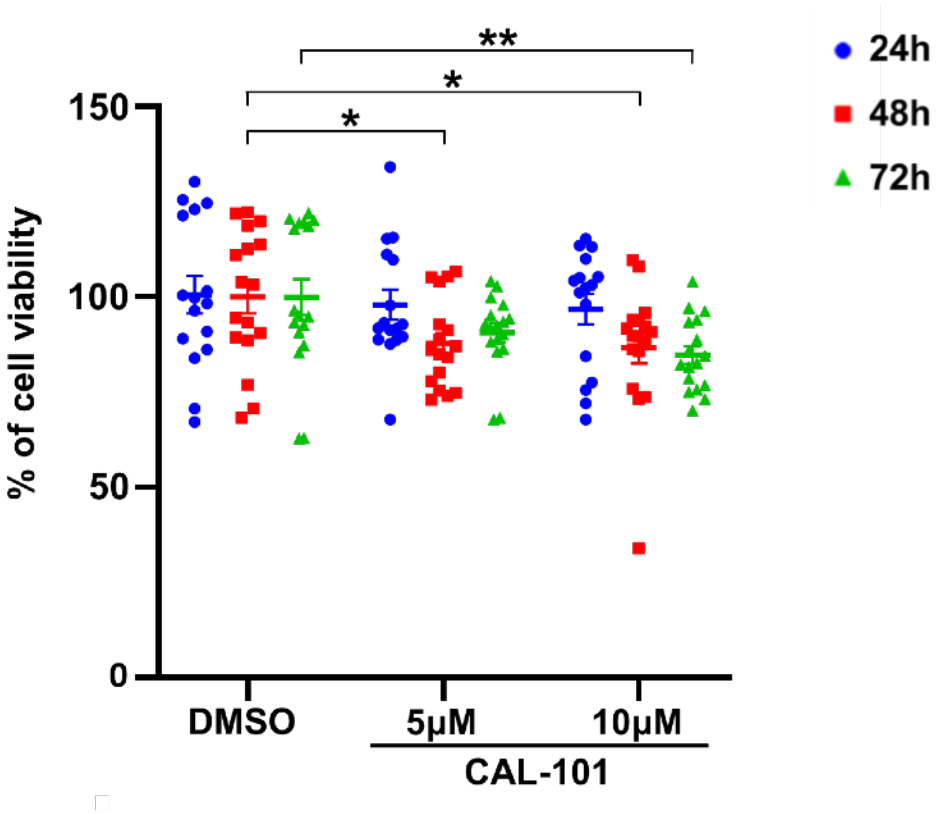

Supplementary Figure 19

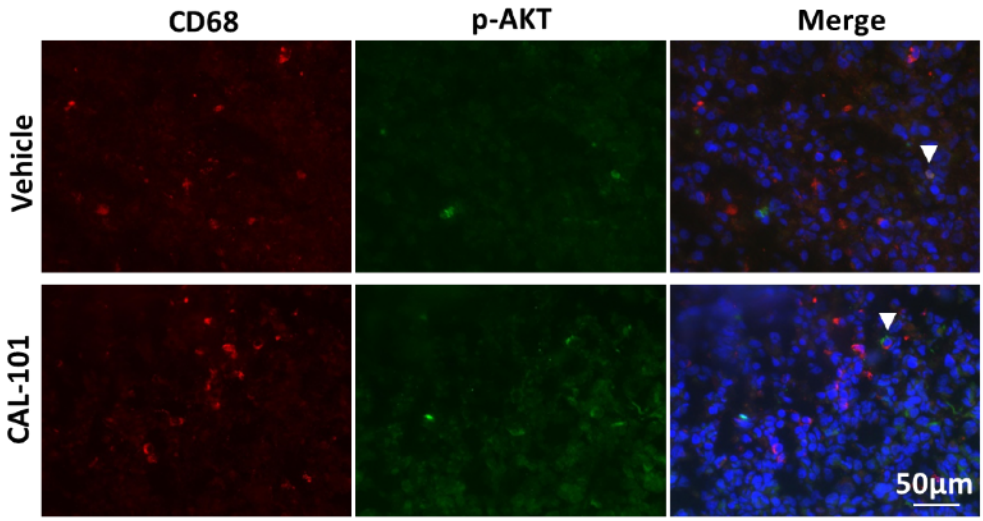

Supplementary Figure 20

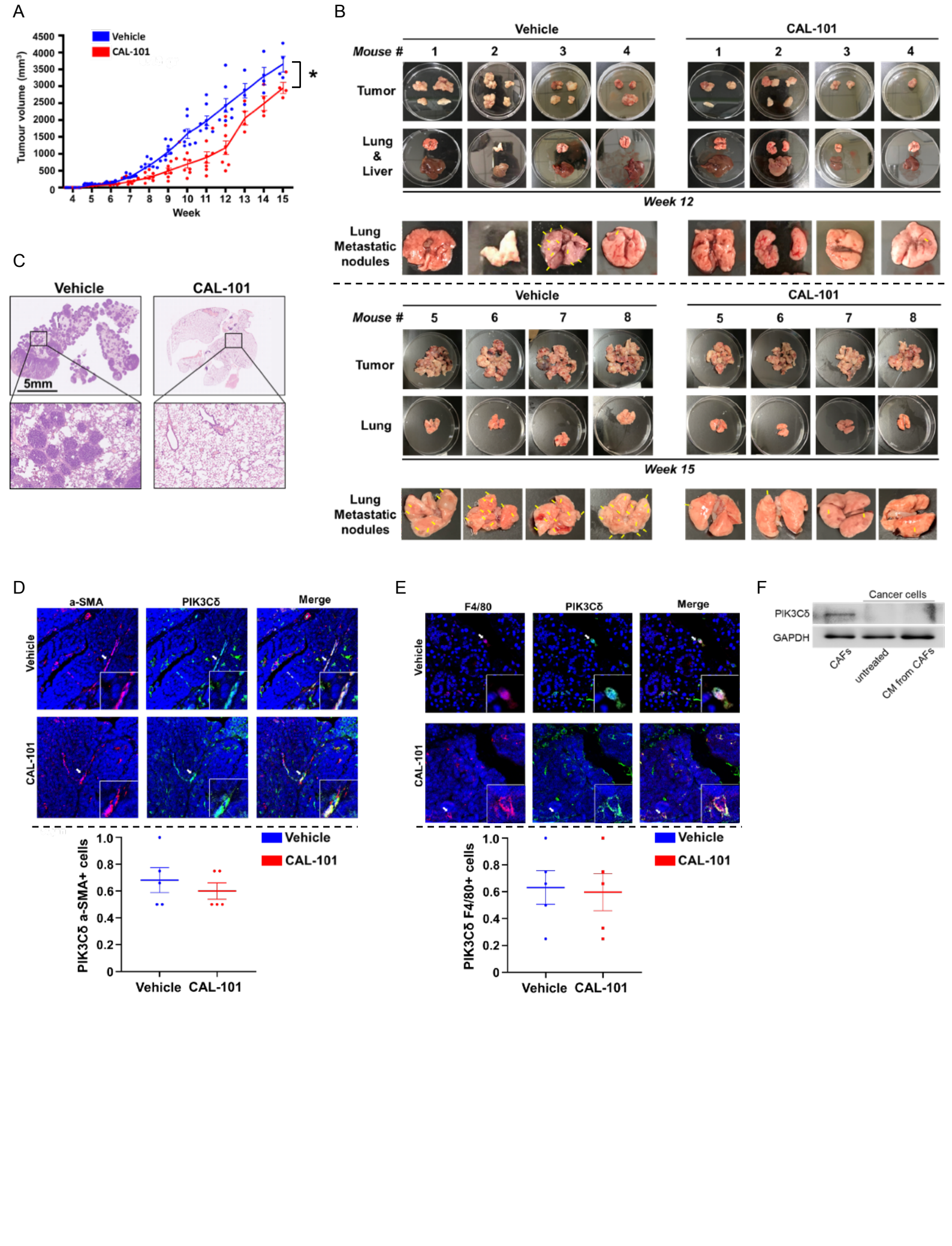

Supplementary Figure 21

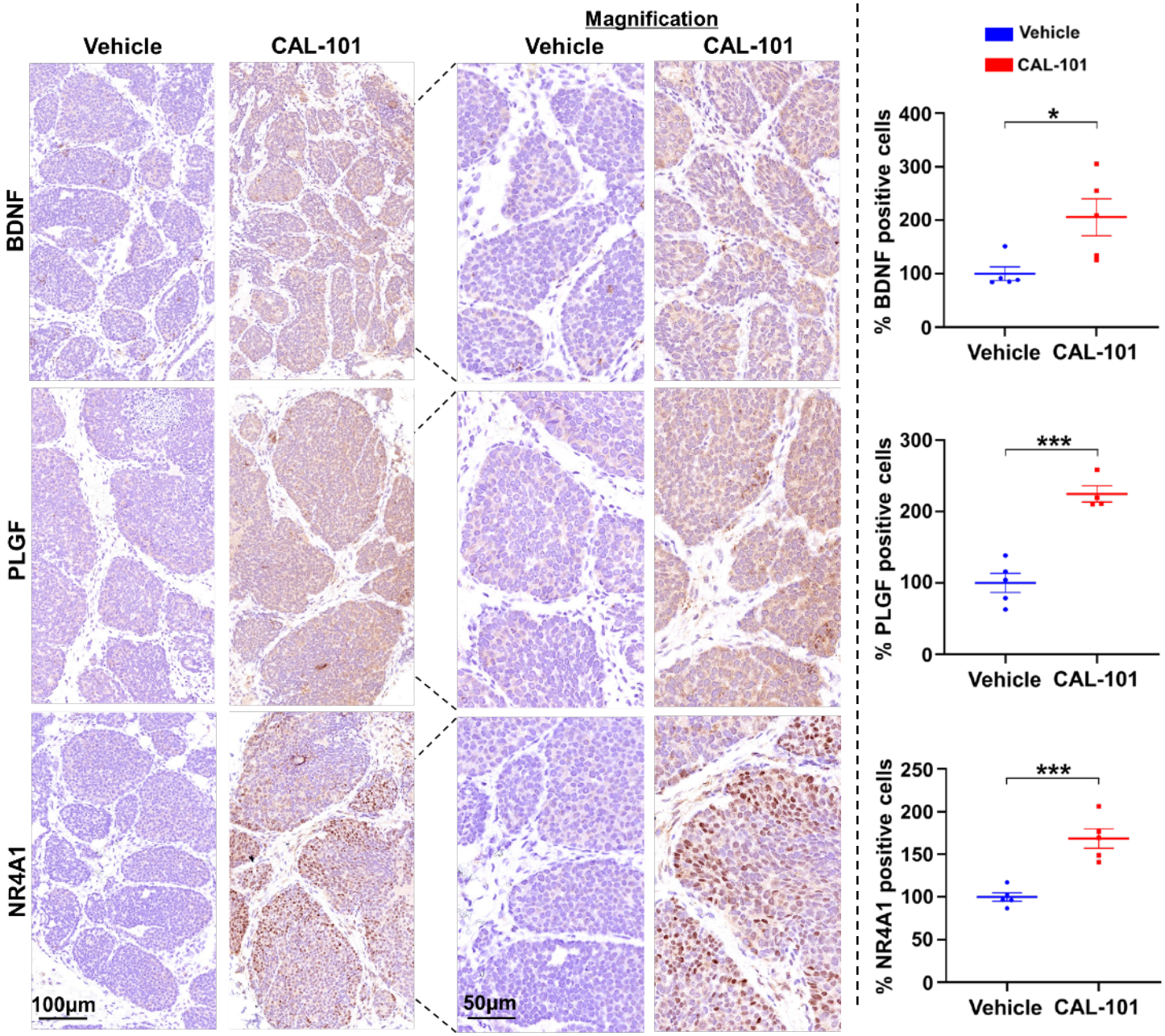

Supplementary Figure 22

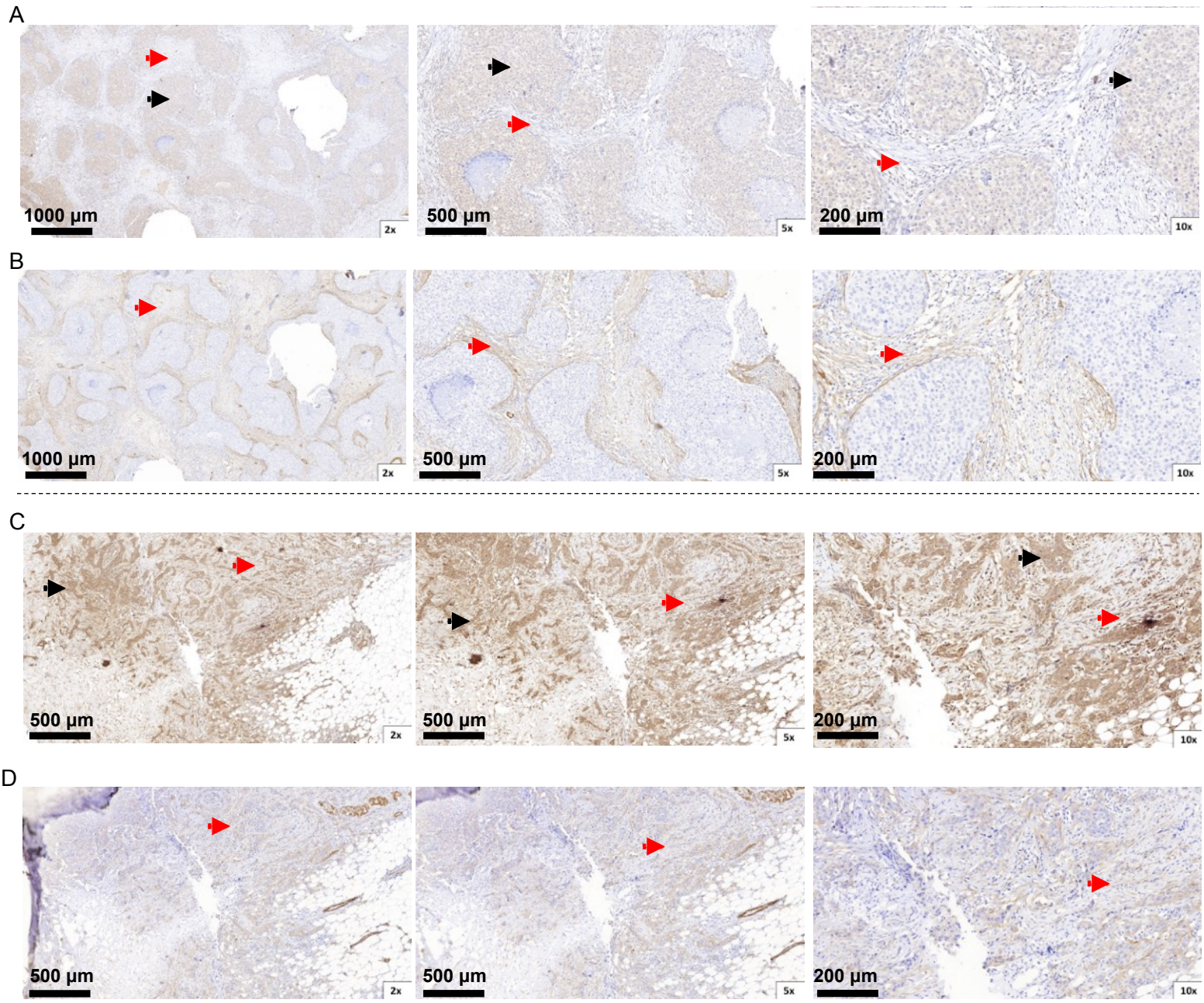

Supplementary Figure 23

A

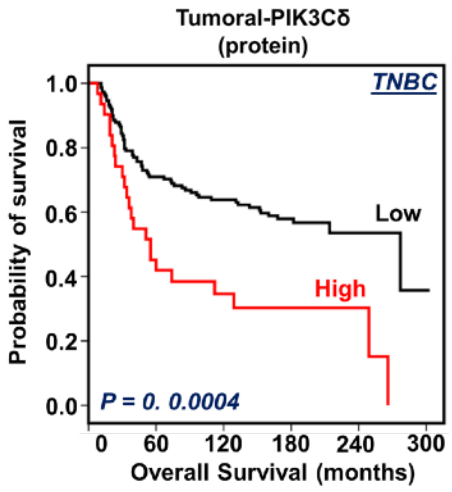

B

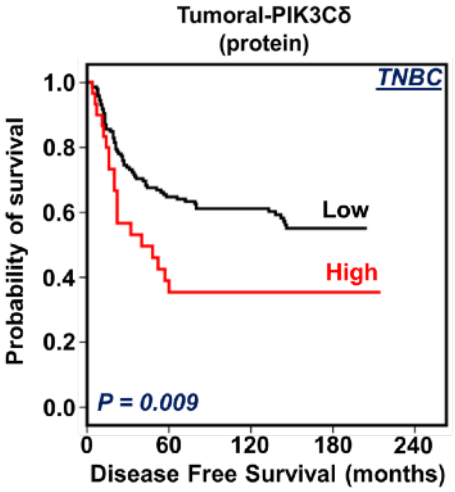

C

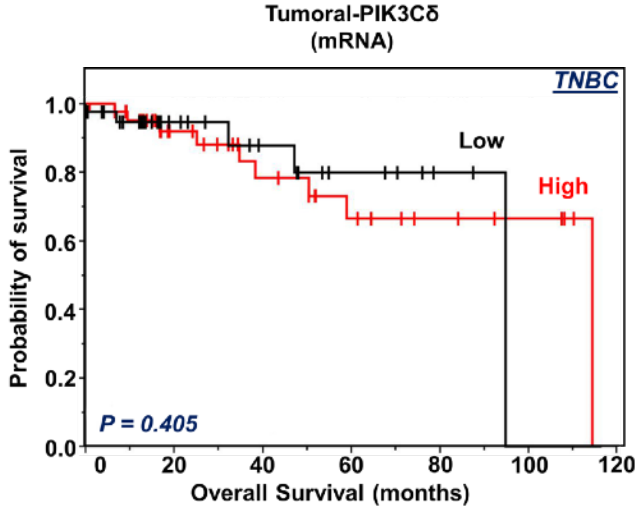

D

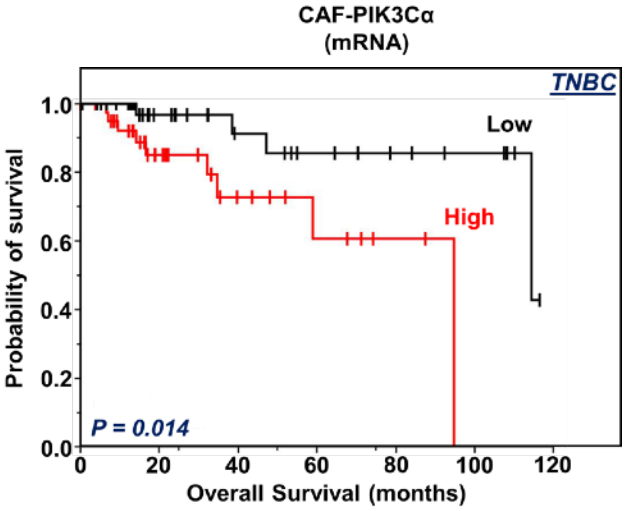

E

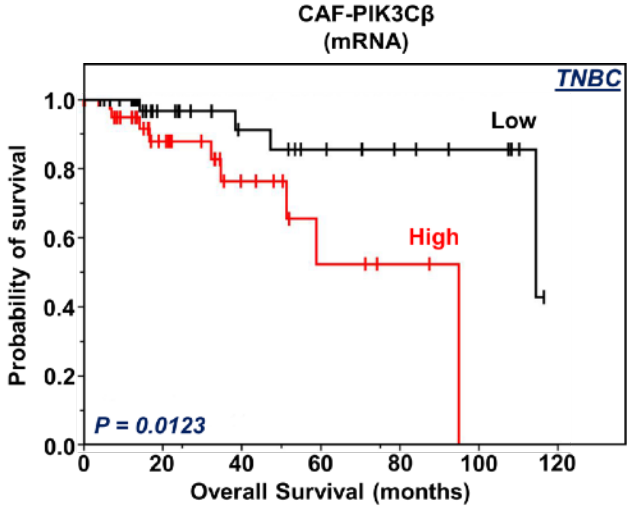

F

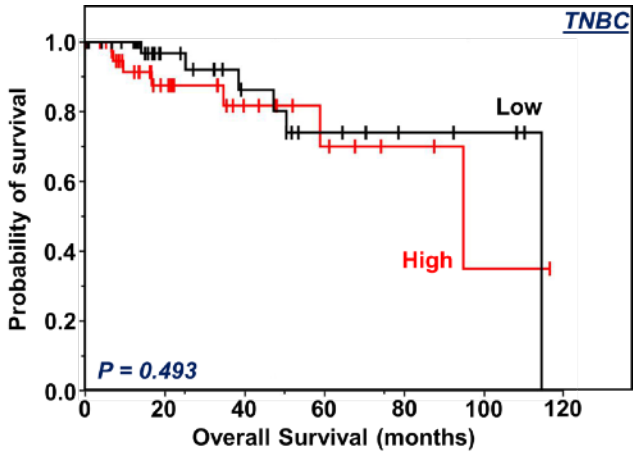

Supplementary Table Legends

Supplementary Table 1. TNBC patients' clinical information from whom the primary fibroblasts were obtained from. Primary fibroblasts were obtained from TNBC patients' specimens. Patients' characteristics including age, tumor type, tumor grade, ER/HER2 status, ER/HER2 score, response to treatment and survival status.

Supplementary Table 2. siRNA Kinome screening results in HMF and MRC5. [A & J] Kinase symbol; [B,C & K] Delta Ratio (replicate 1 or 2); [D] Average of Delta Ratio; [E] Standard deviation calculated from the two Delta Ratios in columns B and C; [F & L] P-Value. [G & M] P value corrected (Bonferroni correction). [H & N] Z score (average).

Supplementary Table 3. Secretome report showing differentially expressed secreted proteins in CAL-101 treated HMF and MRC5 cells. [A & M] RefSeq ID; [B,C & N,O] Ratio of Chemiluminescence signal measured in DMSO or CAL-101 treated cells (replicate 1 & 2). [D,E & P,Q] Normalized value were calculated according to manufacturer's recommendation using value from positive control (replicate 1 & 2). [F,G,H,I & R,S,T,U] Log2 values for the normalized ratio DMSO/DMSO and DMSO/CAL-101. [J & V] Average of the Log2 normalized value of DMSO/CAL101 replicate. [K & W] P-value: Two-sample Student T-Test value to determine whether the DMSO/DMSO and DMSO/CAL-101 are likely to have come from the same two underlying populations that have the same mean.

Supplementary Table 4. DESeq2 report showing differentially expressed genes for comparison model. MDA-MB-231 cells co-cultured with CAL-101 treated vs DMSO treated MRC5 cells. [A] Ensembl ID; [B] Base Mean: Mean of the normalized read counts across all the samples; [C] Log2 fold change: Log2 fold change is the effect size estimate that measures how much gene's expression have changed due treatment with doxorubicin treatment in comparison to treatment with DMSO; [D] LfcSE: Standard error estimate for the Log2 fold change estimate; [E] Stat: Wald-statistics to test whether the data provides sufficient evidence to conclude if the particular effect size estimate value is really different from zero; [F] P value: indicates the probability that a fold change as strong as the observed one, or even stronger, would be seen under DMSO treatment; [G] P adjusted: Benjamini- Hochberg (BH) corrected P values. BH method calculates an adjusted P value for each gene which answers the following question: if we called significant all genes with a P value less than or equal to this gene's P value threshold, what would be the fraction of false positives among them; [H] Symbol: Gene symbol; [I] Entrez: entrez id of each gene.

Supplementary Table 5. Sequences of primers used for the qRT-PCR validation.

Supplementary Table 6. Table showing functional annotation of pathways enriched for CAL-101 regulated secreted proteins. Table displaying the IPA predicted functional categories for pathways enriched with secreted proteins commonly upregulated by CAL-101 treatment of HMF and MRC5 cells.

Supplementary Table 7. Clinico-pathologic parameters of Nottingham series' TNBC patients' cohort.

Supplementary Table 8. Association of fibroblast-PIK3Cδ protein expression with TNBC patients' outcome.

Supplementary Table 9. Association of tumoral-PIK3Cδ protein expression with TNBC patients' outcome.

Supplementary Table 10. Clinico-pathologic parameters of ERα$^+$ patients' cohort from Singapore.

Supplementary Table 11. Association of fibroblast-PIK3Cδ protein expression with ERα$^+$ patients' outcome.

Supplementary Table 12. Association of tumoral-PIK3Cδ protein expression with ERα$^+$ patients' outcome.

Supplementary Table 13. List of BC CAF- and immune marker- genes.

Supplementary References

1. Gagliano T, Gentilin E, Tagliati F, Benfini K, Di Pasquale C, Feo C, et al. Inhibition of epithelial growth factor receptor can play an important role in reducing cell growth and survival in adrenocortical tumors. Biochem Pharmacol. 2015;98(4):639-48.
2. Gagliano T, Bellio M, Gentilin E, Mole D, Tagliati F, Schiavon M, et al. mTOR, p70S6K, AKT, and ERK1/2 levels predict sensitivity to mTOR and PI3K/mTOR inhibitors in human bronchial carcinoids. Endocr Relat Cancer. 2013;20(4):463-75.
3. Dunne PD, McArt DG, Blayney JK, Kalimutho M, Greer S, Wang T, et al. AXL is a key regulator of inherent and chemotherapy-induced invasion and predicts a poor clinical outcome in early-stage colon cancer. Clin Cancer Res. 2014;20(1):164-75.
4. Pfaffl MW. A new mathematical model for relative quantification in real-time RT-PCR. Nucleic Acids Res. 2001;29(9):e45.
5. Tagliati F, Gagliano T, Gentilin E, Minoia M, Mole D, Delgi Uberti EC, et al. Magmas overexpression inhibits staurosporine induced apoptosis in rat pituitary adenoma cell lines. PloS one. 2013;8(9):e75194.
6. Stebbing J, Shah K, Lit LC, Gagliano T, Ditsiou A, Wang T, et al. LMTK3 confers chemo-resistance in breast cancer. Oncogene. 2018.
7. Dobin A, Davis CA, Schlesinger F, Drenkow J, Zaleski C, Jha S, et al. STAR: ultrafast universal RNA-seq aligner. Bioinformatics. 2013;29(1):15-21.
8. Love MI, Huber W, Anders S. Moderated estimation of fold change and dispersion for RNA-seq data with DESeq2. Genome Biol. 2014;15(12):550.
9. LeBleu VS, Kalluri R. A peek into cancer-associated fibroblasts: origins, functions and translational impact. Dis Model Mech. 2018;11(4).
10. Newman AM, Liu CL, Green MR, Gentles AJ, Feng W, Xu Y, et al. Robust enumeration of cell subsets from tissue expression profiles. Nat Methods. 2015;12(5):453-7.
11. Abd El-Rehim DM, Ball G, Pinder SE, Rakha E, Paish C, Robertson JF, et al. High-throughput protein expression analysis using tissue microarray technology of a large well-characterised series identifies biologically distinct classes of breast cancer confirming recent cDNA expression analyses. Int J Cancer. 2005;116(3):340-50.
12. Blamey RW, Ellis IO, Pinder SE, Lee AH, Macmillan RD, Morgan DA, et al. Survival of invasive breast cancer according to the Nottingham Prognostic Index in cases diagnosed in 1990-1999. Eur J Cancer. 2007;43(10):1548-55.
13. McCarty KS, Jr., Miller LS, Cox EB, Konrath J, McCarty KS, Sr. Estrogen receptor analyses. Correlation of biochemical and immunohistochemical methods using monoclonal antireceptor antibodies. Arch Pathol Lab Med. 1985;109(8):716-21.